Electrical stimulation of myelinated axons: An interactive tutorial supported by computer simulation

Simon M. Danner, Cornelia Wenger and Frank Rattay

August 11, 2011

Preprint

Original publication: Danner, S. M., Wenger, C. and Rattay, F. (2011). Electrical stimulation of myelinated axons: An interactive tutorial supported by computer simulation. Saarbrücken: VDM Verlag.

Preface

Recently performed medical research constantly strengthens the concept that electrical stimulation of the nervous system is a promising practical technique for many clinical applications. To name just a few, muscles can be stimulated to avoid disuse, impaired function can be improved by targeted stimulation of certain nerves, neurological pain can be controlled, implants can be used for the deaf and blind to regain perception, and brain and spinal cord function can be researched. Not only the fields of application of electrical stimulation are numerous, also many different approaches exist in order to develop adequate mathematical models for diverse neural structure. These models can be used to calculate, for example, excitation thresholds and action potential propagation and thus offer the possibility to study the electrical stimulation without complicated and possibly invasive experiments.

The main goal is to provide an easily understandable introduction into a complex matter. We focus on the modeling and simulating of the myelinated axon since it has been identified to be the most excitable part to external electrical stimulation while analyzing different substructures of a neuron. Therefore we will explain the main aspects of the derivation of some complex nerve fiber models that describe the influence of the applied electrical field on the neurons. With this fundamental knowledge the reader will be able to appropriately apply these techniques, which is essential to understand the underlying

mechanisms involved in the artificial activation of the central and peripheral nervous system by electrical stimulation. Furthermore an application is presented that allows to experiment with two commonly used axon models. Certain parameters can be varied and thresholds can be calculated. The goal is to provide an application with which students and interested people can learn the properties of electrical stimulation and the differences between commonly used axon models. The application, which can be downloaded for free from `http://code.google.com/p/axonsim/`, is designed to offer as much freedom to the user as possible, in order to enable a learning by experimenting approach.

Contents

Contents **3**

List of Figures **5**

List of Tables **7**

1 Introduction **9**

2 Background **13**

2.1 Anatomy and physiology 13

2.2 Computer models of neurons 14

Formal or abstract spiking models 15

Integrate and fire 15

Izhikevich: A simple model of spiking neurons 16

Hodgkin-Huxley-like or conductance based models 18

2.3 Axon models 25

McNeal model 25

CRRSS model 27

MRG model 30

3 The application **41**

3.1 Implementation and documentation 41

The user interface 43
Implementation remarks 50
Nerve fiber curvature 50
Electrical field 52
Approximation of the activating function 55
Stimulation functions 55
Binary search 56
ODE solver 58
3.2 Examples 58
Propagation of an action potential 59
Intracellular- and extracellular stimulation 59
The CRRSS and the MRG model 61
Activation threshold and fiber diameter 64
Activation threshold and fiber curvature 65
Activation threshold and electrode-fiber distance 67
Stimulation functions 67

4 Summary **75**

Bibliography **77**

List of Figures

2.1 The Izhikevich model for spiking neurons. 17
2.2 Equivalent circuit of the Hodgkin-Huxley model. 19
2.3 Simulation of the original Hodgkin-Huxley model from 1952 with current injection. 21
2.4 The equivalent circuit of the McNeal model. 26
2.5 The equivalent circuit of the CRRSS model. 28
2.6 Visualisation of the geometry and the compartments of the MRG model. 31
2.7 Equivalent Circuit for the MRG axon model. 39

3.1 The user interface of AxonSim 44
3.2 Illustration of the method to create curved fibers. 51
3.3 Potential distributions evaluated along a straight fiber 20 mm long fiber. 54
3.4 Example of an action potential propagation. 60
3.5 Example of intracellular stimulation. 62
3.6 Simulation of the CRRSS model. 63
3.7 Influence of the fiber diameter on the activation threshold for extracellular stimulation. 64
3.8 Influence of the fiber curvature on the activation threshold. 66

3.9 Influence of the electrode to fiber distance on the potential distribution and activating function. 70
3.10 Influence of the electrode to fiber distance on the potential distribution and activating function. 71
3.11 Example of a custom stimulation function. 72
3.12 Example of a custom stimulation function specified by a function file. 73
3.13 Illustration of the effect of 10 kHz stimulation with en extracellular electrode. 74

List of Tables

2.1 Parameters of the CRRSS model 30
2.2 MRG model electrical parameters 32
2.3 MRG model geometric parameters 40

Chapter 1

Introduction

An applied electrical field can be used to artificially stimulate the nervous system. There are numerous medical and scientific applications for the electrical stimulation of the nervous system. Inactive muscles can be repetitively activated in order to prevent muscular atrophy due to disuse (Dimitrijevic and Dimitrijevic, 2002), impaired movement function can be enhanced, e.g. with the stimulation of the peroneal nerve of a person with foot drop (Liberson, Holmquest, Scot, and Dow, 1961), the central nervous system (CNS) function can be researched (e.g. Minassian, Persy, Rattay, Dimitrijevic, Hofer, and Kern, 2007), and many more applications exist.

Computer simulation of the electrical stimulation of the nervous system often accompanies research of functional electrical stimulation methods, biomedical engineering and neuromodulation (Rattay, Greenberg, and Resatz, 2003), e.g. for spinal cord stimulation (Coburn, 1985; Rattay, Minassian, and Dimitrijevic, 2000; Danner, Hofstoetter, Ladenbauer, Rattay, and Minassian, 2011; Száva, Danner, and Minassian, 2011) and deep brain stimulation (McIntyre, Grill, Sherman, and Thakor, 2004; Rattay and Wenger, 2010), since the effects of the artificial intra- and extracellular stimulation can be simulated using computer models based on the work of Hodgkin and Huxley (1952).

For people who use or want to simulate the stimulation of the nervous

system, it is important to understand the mechanisms involved. Thus an application, which can be used to teach and learn the influence of intra- and extracellularly applied electrical fields on the nervous system is presented in this thesis. The analysis of different substructures of a neuron has shown that the part most excitable by external electrical stimulation is the myelinated axon. Due to the high value of the membrane capacitance of the soma compared to that of the non-myelinated node of Ranvier, the probability to excite a nerve at the soma region is low (Porter, 1963; Nowak and Bullier, 1998; Rattay, 1998, 1999). Myelinated fibers are more excitable than unmyelinated ones and large-diameter fibers have lower thresholds than the thinner ones (Ranck, 1975; Rattay, 1987, 1990; Roth, 1994). It should be noted that the relationship between excitation threshold and the fibre diameter is not linear. Thresholds drastically increase for small-diameter fibers (Veltink, van Alsté, and Boom, 1988; Struijk, Holsheimer, and Boom, 1993; Wenger, Paredes, and Rattay, 2011). Thus the emphasis of the application is on the electrically stimulated axon.

The complex and theoretical nature of the topic can be simulated and illustrated, and thus an interactive approach for learning and teaching seems optimal, but until now no adequate interactive application exists that can be easily used to simulate the effects of electrical stimulation of the myelinated axons. Therefore the goal of this work is to offer an application that can be used to teach and learn: *(i)* the effects of intra- and extracellular stimulation, *(ii)* the conducting properties of myelinated axons and *(iii)* the differences between the most commonly used models. The application should be useable as a supplement to a course, as well as a self contained package to learn without supervision. An optimal learning outcome shall be secured by giving the incentive to experimentally interact with the stimulation settings.

To give a good overview of the tools available to simulate extracellular stimulation, the application (Danner, 2011) is able to calculate the activating function (Rattay, 1986, 1988, 1989), which can be used to approximate the

influence of extracellular stimulation (see chapter 2 for details), and simulate following axon models, which are applicable also for the human case:

- CRRSS model (Chiu, Ritchie, Rogart, and Stagg, 1979; Sweeney, Mortimer, and Durand, 1987)
- MRG model (McIntyre, Richardson, and Grill, 2002)

The CRRSS model is an adaptation of the McNeal model for mammalian myelinated nerve fibers and is widely used, but has been shown to overestimate threshold values (Wesselink, Holsheimer, and Boom, 1999). The MRG model is a double cable model with a detailed reproduction of the ion channels and the anatomy of the nerve fiber. Further Kuhn, Keller, Lawrence, and Morari (2009) have shown that the MRG model realistically reproduces the threshold values for transcutaneous electrical stimulation.

Different cases can be selected, i.e. variations of intracellular stimulation and extracellular stimulation with point electrodes. Most parameters, i.e. stimulation strength, pulse shape, distance of the electrode, etc., are changeable by the user to investigate their effects. In combination with the documentation the user should be able to understand the underlying concepts and will get familiar with the computer simulation of electrically stimulated nerve fibers.

This thesis consists of two main parts:

- Chapter 2 explains in detail the anatomy and physiology of nerve cells, how they can be stimulated and how neuron models in general and axon models in detail work.
- Chapter 3 deals with the implementation and documentation of the application and illustrates fundamental properties of neurons under the influence of an electrical field with the help of examples using the presented application.

Chapter 2

Background

In the following paragraphs the biological background is summarized and an introduction into neuron and nerve fiber models is given. Three models of myelinated axons are described in detail.

2.1 Anatomy and physiology

The nervous system mainly consists of nerve cells (neurons) and glia cells, which provide support, nutrition and with the help of myelin improve the speed of action potential propagation (Bear, Connors, and Paradiso, 2001). Neurons consist of many parts, but most important for the simulations of the membrane potentials are the soma, the dendrites, the axons and the synapses. The soma is the main cell body. The dendrites are the projections of the neuron that act as a site of synaptic contacts of other neurons. The axons are longer projections that conduct the action potential to other cells and the synapses are the electrochemical connections on the end of an axon to another cell (Kandel, Schwartz, and Jessell, 2000).

The membrane of the neuron is tightly structured and thus prevents ions from passing through, but even at rest there is small conductivity (Pfützner, 2003). There are different ion concentrations on the extracellular and intracel-

lular parts of the neuron that are held constant by energy consuming ion pumps (Bear et al., 2001). When the membrane potential—the potential between the inner and outer part of the membrane—exceeds a certain threshold, sodium gates open and Na^+ ions flow into the cell and a depolarization occurs shorty after potassium channels open and K^+ ions flow out of the cell to counteract the depolarization. After a short period of hyperpolarization the membrane potential returns to its initial state (Pfützner, 2003). This is called an action potential. These action potentials travel along the axons and are propagated through the synapses to different neurons (Bear et al., 2001). The resting state is usually at about -70 mV and during depolarization an about 100 mV higher value is reached. The action potentials travel along the neuronal membrane and are propagated to the next cell via the synapses. The main computational property is believed to be the membrane potential of the neurons. There exist many different types of neurons, neurons that generate excitatory or inhibitory post synaptic potentials (potentials that are generated by the pre-synaptic neuron and influence the post-synaptic neuron), bursting neurons, chattering neurons, resonating neurons and many more (Dayan and Abbott, 2001).

2.2 Computer models of neurons

The majority of artificial neural network models are based on the propagation of continuous variables from one processing unit or 'neuron' to the next (Maass and Bishop, 2001). However, real neurons do not work like that. Simplistically speaking, neurons operate with discrete events, so called action potentials or spikes. Further the frequency and timing of these action potentials play an important role in their computational capabilities (Izhikevich, 2007). With the work of Hodgkin and Huxley (1952) on the quantitative properties of the squid axon, the simulation of excitation of a single neuron became possible. And with increasing computational power and insight from neuroscience more complex

models of neurons and networks became available (Dayan and Abbott, 2001). The motivation of these simulations is twofold, on one side it is the desire to enhance our understanding of information processing in biological networks and on the other side it is the goal creating new information processing technologies (Maass and Bishop, 2001). Here we are interested in the former.

Formal or abstract spiking models

A possibility, besides modeling detailed membrane dynamics, is to use abstract models that capture certain properties that are of interest.

Integrate and fire

One such model is the integrate and fire (IF) model that dates back to 1907 and was first described by Lapicque (1907). It consists of a single capacitor that represents the membrane. And with additional current—either through post synaptic potentials or through artificial stimulation—the membrane potential changes from its rest potential and when a certain threshold is exceeded the potential will be reset and an action potential is assumed to be generated. The model does not generate a spike by itself, it just consists of the discharge of a capacitor. The equations can be written as

$$\frac{dV^m}{dt} = -I^{inj}/c \tag{2.1}$$

where V^m is the membrane potential, i.e. the potential difference between extra- and intracellular milieu, I^{inj} is the injected current and c the capacity of the membrane.

The timing of spike generation can be used as post synaptic potentials for other neurons. The post synaptic potentials are mostly defined by a synaptic weight and a simple time dependence (e.g. alpha-functions). With these models it is already possible to construct large scale networks and observe their dynamic properties.

An extension of the IF model is the leaky integrate and fire model that adds a resistor in parallel to the capacitor and introduces time dependency of the input. In other words postsynaptic potentials are not just summed up, they are also decaying if the threshold is not reached. Thus spike timing becomes important with this model. The model equation is

$$\frac{dV^m}{dt} = -(I^{inj} + g(V^m))/c \tag{2.2}$$

where g is the conductance of the membrane.

Both models are subject to a low computational cost and are easily applicable to large scale networks, but lack many properties of the Hodgkin-Huxley like neurons. For example real neurons do not produce all or nothing signals, action potentials can be of different size, they do not sum up input signals, rather they are resonators that respond to certain frequencies better than to others and finally there is no exact threshold (Izhikevich, 2006, 2007). All these features are incorporated into the Hodgkin-Huxley models due to their exact replication of the ion dynamics, but are neglected in the IF and leaky-IF models. Moreover the simulation of axons and action potential propagation along axons is not possible with such models.

In the next subsection a model is described that captures many different properties of the Hodgkin-Huxley neurons but still remains a low computational cost.

Izhikevich: A simple model of spiking neurons

The Izhikevich (2003) model can replicate a wide variety of different neuronal behavior that occurs in the central nervous system. It is a result of mathematical analysis of the Hodgkin-Huxley and other models and reproduces many of their properties. The model equations are listed in listing 2.1.

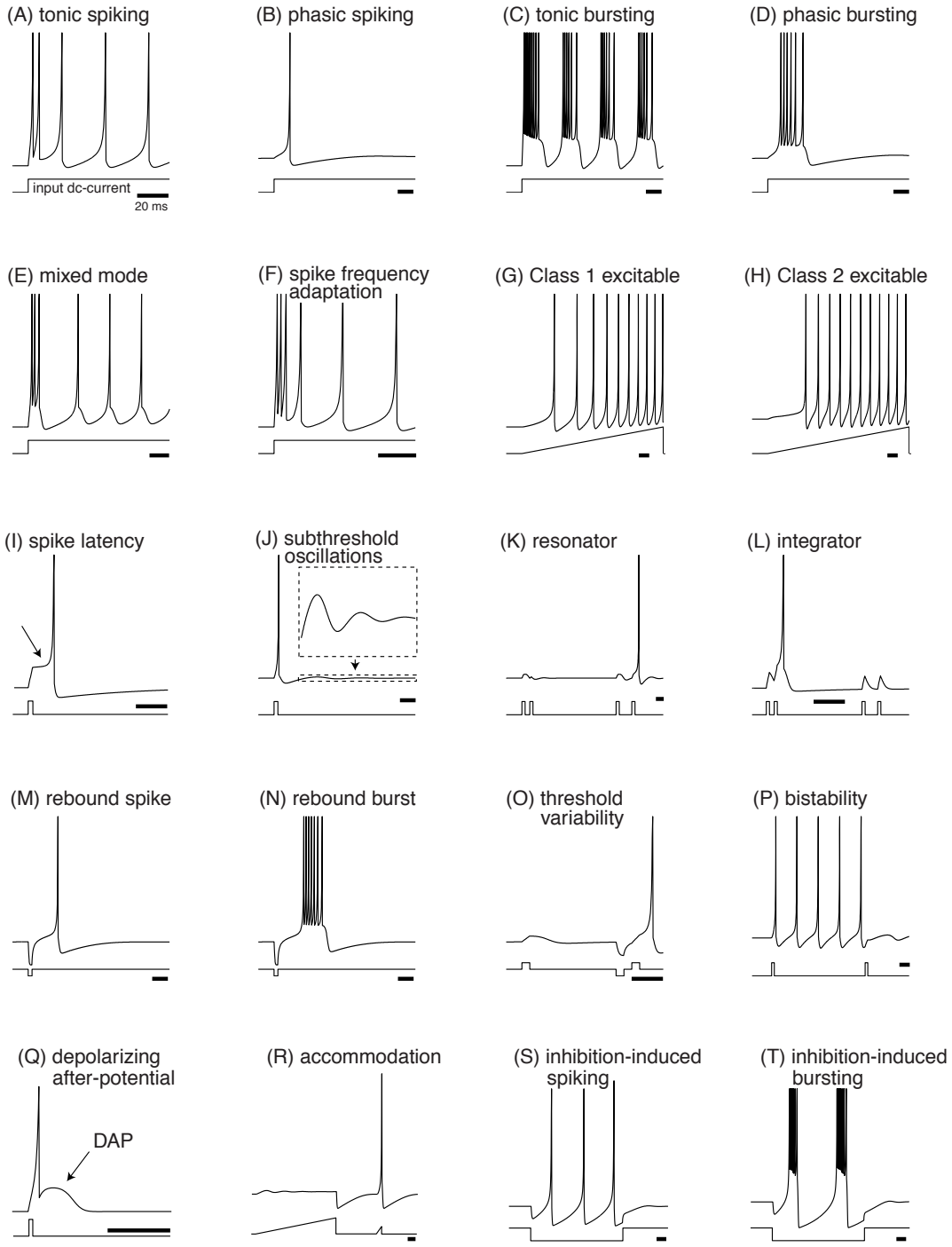

Figure 2.1: Examples of neurons modeled by the Izihkevich model. Electronic version of the figure and reproduction permissions are freely available at `www.izhikevich.com`.

Listing 2.1: Equations of the Izhikevic model.

```
v'=0.04v^2+5v+140-u+I
u'=a(bv-u)

if v == 30mV
    v=c, u=u+d
```

The model still works with a resetting mechanism (like the IF/LIF model) when the threshold of 30 mV is surpassed. It can be solved by forward Euler integration with a step size of 1 ms and thus has a very low computational cost. By setting the parameters (a, b, c and d) a large number of different behaviors of neurons can be reproduced (see figure 2.1). It is well suited for simulation of large scale networks with various kinds of neurons but simulation of the extracellular influence is not easily possible.

In the following section a class of neuron models is discussed that simulates the ion channels of the neuronal membrane and produce a realistic dynamic behavior of the membrane potential of neurons.

Hodgkin-Huxley-like or conductance based models

Hodgkin and Huxley (1952) were the first to quantitatively describe the membrane potential of neurons including the simulation of ion channels. Their work was based on the squid axon with large diameters and was thus easier to investigate than other axons. With the patch clamp technique—a method where the current influx of ion channels at a constant voltage can be measured—equations for different ion channels could be deduced. With a minimal set of two channels, i.e. potassium and calcium, in combination with a leakage conductance and a capacitance in parallel an action potential can be produced, the equivalent circuit can be seen in figure 2.2.

With the aid of the equivalent circuit (figure 2.2) the equations can be deduced using Kirchoff's law, which states that the sum of current influx is equivalent to the sum of current efflux or in other words, when influx is seen

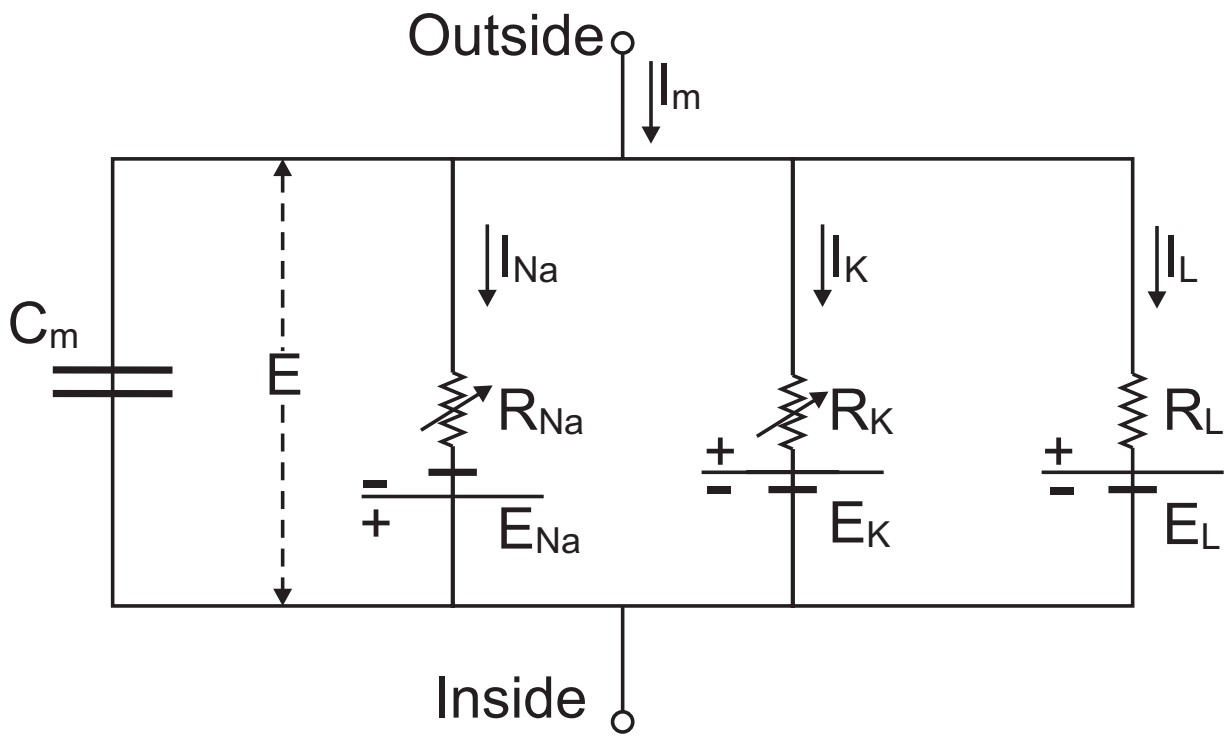

Figure 2.2: Equivalent circuit of the Hodgkin-Huxley model including a leakage conductor, a capacitor, and two active membrane channels (potassium and sodium). R denotes the maximal resistance, C the capacity and E the reversal potential. Adapted from Hodgkin and Huxley (1952).

as positive and efflux as negative current flow, it states that the sum of the current flux at one point is 0:

$$\sum I = 0. \tag{2.3}$$

The equation for the conductance (i.e. leakage current) can be written as:

$$I^{lk} = g^{lk} \cdot (V^m - E^{lk}) \tag{2.4}$$

where g^{lk} is the conductance, V^m is the membrane potential, E^{lk} is the reversal or Nernst potential and I^{lk} is the resulting current flux. For the capacitance the equations are given as follows:

$$I^c = \frac{dV^m}{dt} \cdot c \tag{2.5}$$

where c is the capacitance, I^c is the current flux of the capacitor and t is the time. Substituting the equations of the active ion channels with I^{active} results in:

$$I^{active} + g^{lk} \cdot (V^m - E^{lk}) + \frac{dV^m}{dt} \cdot c = 0. \tag{2.6}$$

Using equivalent transformations the equation can be written as follows:

$$\frac{dV^m}{dt} = -(I^{active} + g^{lk} \cdot (V^m + E^{lk}))/c. \tag{2.7}$$

In this form the equation represents an initial value problem and can be easily solved using numerical integration methods (i.e. forward or backward Euler or more complex methods if necessary).

The active channels are described in a voltage dependent way using the same equation as the leakage conductance, but substituting the constant conductance g with a time and voltage dependent conductance $g(t, V)$

$$g(t, V^m) = \bar{g} \cdot \prod_i m_i(t, V^m)^{p_i} \tag{2.8}$$

where $\bar{g}$ is the maximal conductivity of the ion channels, p_i is an integer and m_i is the solution of a differential equation of the form:

$$\frac{dm(t, V^m)}{dt} = \frac{m_\infty(V^m) - m(t, V^m)}{\tau_m(V^m)} \tag{2.9}$$

$$= \alpha_m(V^m) \cdot (1 - m) - \beta_m(V^m) \cdot m. \tag{2.10}$$

The parameters α and β for all m are determined experimentally with patch and voltage clamp methods and differ between cell types and ion channels.

In figure 2.3 the simulation of the original Hodgkin-Huxley model is depicted. The model is excited by injection of a current. It can be seen how the interplay between the ion channels generate the action potential including de- and hyperpolarization.

Note that a neuron in this simulation is abstracted to be homogenous and not having any axons or dendrites and thus is simulated as a single set of

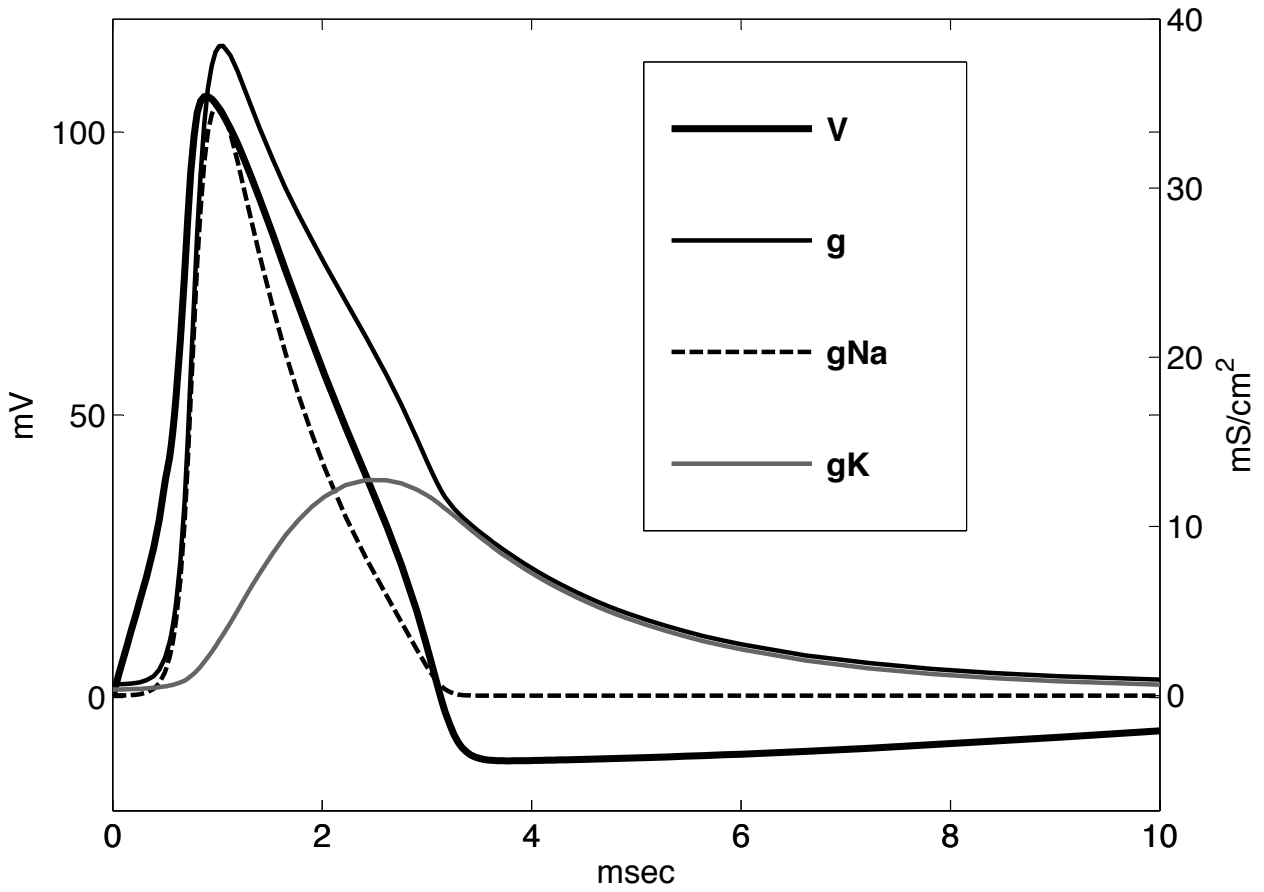

Figure 2.3: Simulation of the original Hodgkin-Huxley model from 1952 with current injection. The change of voltage from the resting potential and the change of conductance due to the influence of the ion channels is depicted. Adapted from Hodgkin and Huxley (1952).

equations. When one wants to take into account the propagation of action potentials along the dendrites and axons and incorporate different geometric structures this approach has to be extended.

This can be done by compartmentalization and using the cable theory (Dayan and Abbott, 2001; Niebur, 2008). The cable theory describes how current flows along a cable. Neurons can be seen as branching cables and thus the cable theory can be applied to calculate the current flux between different parts of the neurons. A neuron can be divided into several parts—so called compartments—to account for geometric variations within the neurons, i.e. differences between the soma, dendrites and axons. Each compartment has different geometric properties and is numerically treated as an isopotential element. If the compartments are small enough a sufficiently close approximation of the electrical phenomena in a complex neuron or axon can be described (Rattay et al., 2003). Each compartment can be connected to n other compartments. To do this, intracellular current flux is modeled into the main equation, resulting in:

$$\frac{dV^m}{dt} = -\left(I^{active} + g^{lk} \cdot (V^m - E^{lk}) + \sum_n I_n^{int}\right)/c \tag{2.11}$$

where I^{int} represents the current influx from compartment n and is given by:

$$I_n^{int} = \frac{E_k^i - E_n^i}{(R_k + R_n)/2)} \tag{2.12}$$

for every compartment n that is connected to compartment k, where E^i is the intracellular voltage measured against the ground—in the special case of no extracellular potential influences and no additional structural modeling it is equivalent to the membrane potential V^m.

With these tools available one can model any kind of neurons if enough knowledge about the makeup of the neuron is known (i.e. ion channels, structure, conductance etc.; De Shutter, 2010). This enables scientists to model

structures present in the brain, with the only limit being the knowledge available of these structures. Thus dynamic properties can be investigated without conducting time consuming and possibly inversive in-vitro experiments.

When considering network models, these kinds of models are most useful for small neural networks where many properties are known (Calabrese and Prinz, 2010). Such models have a high computational cost (Izhikevich, 2003) and if not much is known about the properties of the neurons that one wants to simulate only the most common and general properties of the neurons can be assumed as true and thus little additional information is gained by using complex Hodgkin-Huxley-like models.

In the case of the extracellular stimulation of the nervous system—the case treated here—models based on Hodgkin and Huxley (1952) dynamics are the most useful. Because the large diameter myelinated axons are the most excitable parts of the nervous system (see chapter 1) simulations often neglect the soma and non-myelinated parts of the neuron, e.g. branchings before the synaptic connections. In the simplest case a model of a myelinated axon consists of two different compartments, one for the node of Ranvier and one for the myelinated internode, alternately chained together. The compartment of the node of Ranvier contains a series of ion channels in parallel to the leak conductance and a capacitance. It is not covered in myelin, in contrary to the internode, whose ion channels—due to their scarcity—are usually neglected. The internode is thus modeled simply as a capacitance in parallel with a conductance, taking into account the special electrical properties of the myelin. It should be noted that more complex models exist that model more complex geometrical properties of the axon and also include ion channels along the internode (see section 2.3; Halter and Clark, 1991; McIntyre et al., 2002).

Here we are interested in the adequate description of the complex, nonlinear behavior of the membrane potential, under the influence of a time varying electrical field (Rattay and Aberham, 1993). It is possible to approximate the

influence of the electrical field on the axon. This can be done with the activating function (Rattay, 1986, 1988, 1989, 1990, 1999). The activating function f_n for compartment n is the driving term of the external potential, or the equivalent injected current:

$$f_n = 1/c \left(\frac{V^e_{n-1} - V^e_n}{R_{n-1}/2 + R_n/2} + \frac{V^e_{n+1} - V^e_n}{R_{n+1}/2 + R_n/2} + ... \right) \tag{2.13}$$

where V^e is the extracellular potential, c the membrane capacity and R the axial resistance.

The activating function represents the rate of membrane voltage change if the neuron is in resting state before the stimulation. Its physical dimensions are V/s or mV/ms, respectively. Put into other words it represents the slope of the membrane voltage at the beginning of the stimulation (Rattay et al., 2003). Following McNeal (1976)'s simplifications for long fibers of an ideal internode membrane, with both membrane capacity and conductance assumed to be 0 the equation for each node is:

$$\frac{dV^m_n}{dt} = \left[-i_{ion,n} + \frac{d\Delta x}{4p_i L} \cdot \left(\frac{V^m_{n-1} - 2V^m_n + V^m_{n+1}}{\Delta x^2} + \frac{V^e_{n-1} - 2V^e_n + V^e_{n+1}}{\Delta x^2} \right) \right] /c \tag{2.14}$$

where d is the constant fiber diameter, Δx the node-to-node distance, L the node length ρ_i the axomplasmatic resistivity, c the capacity and i_{ion} the ionic currents. From this the activating function follows as:

$$f_n = \frac{d\Delta x}{4\rho_i Lc} \frac{V^e_{n-1} - 2V^e_n + V^e_{n+1}}{\Delta x^2}. \tag{2.15}$$

In this case the activating function is proportional to the second order spatial difference of the extracellular potential along the fibers. When $L = \Delta x$ and $\Delta x \to 0$ (2.15) is:

$$f = \frac{d}{4\rho_i c} \cdot \frac{\delta^2 V^e}{\delta x^2} \tag{2.16}$$

and is proportional to the second order spatial differential along the fiber. Positive values of f suggest a depolarization of the membrane potential and negative values a hyperpolarization of the membrane potential. Generally speaking,

since f corresponds to the second order spatial differential of the extracellular potential along the fiber, its curvature induces a change in membrane potential. Thus, the curvature of the fiber, the makeup of the electrical field and transitions between medias of different conductivities influence the excitability of nerve fibers. The effect of fibre bending is well known from cortical stimulation. Sharp changes of the fibre direction of pyramidal cells in the motor cortex result in spike initiation at the sites of the bends when electrical (Iles, 2005; Wongsarnpigoon and Grill, 2008) or magnetic stimulation is applied (Maccabee, Amassain, Eberle, and Cracco, 1993; Iles, 2005; Amassian and Maccabee, 2006). All the mentioned effects will be illustrated using the presented learning tool, AxonSim, in chapter 3.2.

2.3 Axon models

In the following subsections three different axon models will be described, first the model by McNeal (1976), which marks the first attempt to efficiently model an extracellularly stimulated axon. Followed by the CRRSS (Chiu et al., 1979; Sweeney et al., 1987) and the MRG model (McIntyre et al., 2002), the former a widely used model for the mammalian nerve fiber and the latter a recent, detailed model of the axon geometry and ion channels.

McNeal model

The nerve fiber model of McNeal (1976) was a milestone in computer modeling and simulation in biomedical engineering. It was the first spatial model of an axon stimulated by an external point source using a network consisting of a set of local models (Rattay and Aberham, 1993).

The model was constructed using the following assumptions: *(i)* the fiber is infinitely long, *(ii)* the nodes of Ranvier are equally spaced, *(iii)* inernodal distance and axon diameter are proportional to the fiber diameter, *(iv)* the

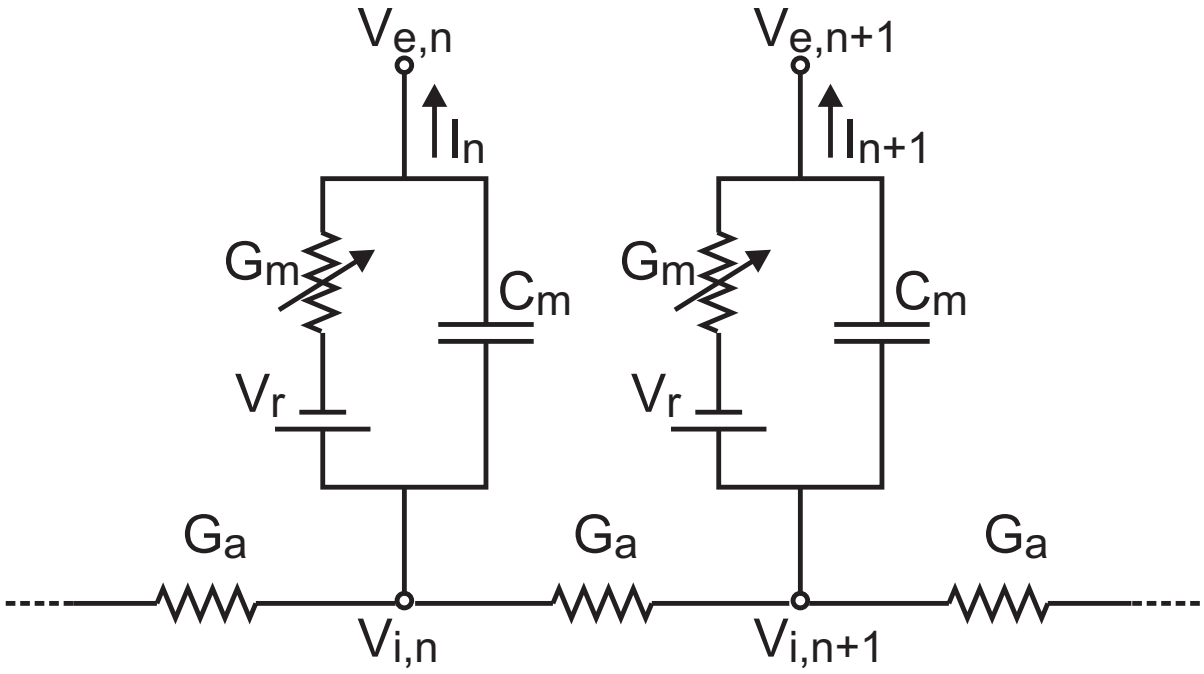

Figure 2.4: The equivalent circuit of the McNeal model. Note that only the membranes of the nodes of Ranvier are modeled, myelin is assumed as a perfect isolator (adapted from McNeal, 1976).

nodal gap is constant for all fiber diameters and *(v)* the myelin is a perfect isolator. Thus, the model simulates only the nodes of Ranvier as isopotential compartments that are connected with a conductance with the neighboring nodes. The nodes of Ranvier are modeled using Frankenhaeuser and Huxley (1964) membrane dynamics that have been derived from the frog axon. The equivalent circuit can be seen in figure 2.4. The membrane current of the node of Ranvier can be described by

$$\frac{dV^m}{dt} = [G^a(E^i_{n-1} - 2E^i_n + E^i_{n+1}) - I^n_n]/c \tag{2.17}$$

where G^a is the axonal conductance and

$$I^n = G^m(V^m - V^r) \tag{2.18}$$

were G^m is the sum of the conductance as specified by the ion channels modeled by Frankenhaeuser and Huxley (1964) and V^r is the reversal potential. All the equations and parameters can be found in McNeal (1976) and Frankenhaeuser and Huxley (1964).

Since in this work we are interested in simulating human or mammalian nerve fibers and this model is based on the frog, it is not used in AxonSim but mentioned here due to its importance in the development of nerve fiber models.

CRRSS model

The Chiu-Ritchie-Rogart-Stagg-Sweeney (abbreviated to CRRSS; Chiu et al., 1979; Sweeney et al., 1987) is a widely used nerve fiber model to simulate the mammalian axon. It is similar to the McNeal (1976) model but removes the assumption that myelin is a perfect isolator and introduces a conductance and capacity of myelin. Thus, the model consists of two different compartments, one for the node of Ranvier and one for the internode, that are alternatingly chained together. An illustration of the equivalent circuit can be seen in figure 2.5.

Each compartment, whether node of Ranvier or internode, can be modeled as specified in (2.11) and (2.12). The influence of the extracellular potential can be written as:

$$I^{ext} = \sum_n \frac{V_n^e - V_k^e}{R_a}. \tag{2.19}$$

Thus, each compartment is given by:

$$\begin{aligned} \frac{dV^m}{dt} \cdot c = -I^{active} - g^{lk} \cdot (V^m - E^{lk}) - \sum_n \frac{E_n - E_k}{R_a} \\ - \sum_n \frac{V_n^e - V_k^e}{R_a} \end{aligned} \tag{2.20}$$

where n is the count of connected compartments, c is the membrane capacity and R_a the axonal resistance of the k-th compartment. Their values depend on

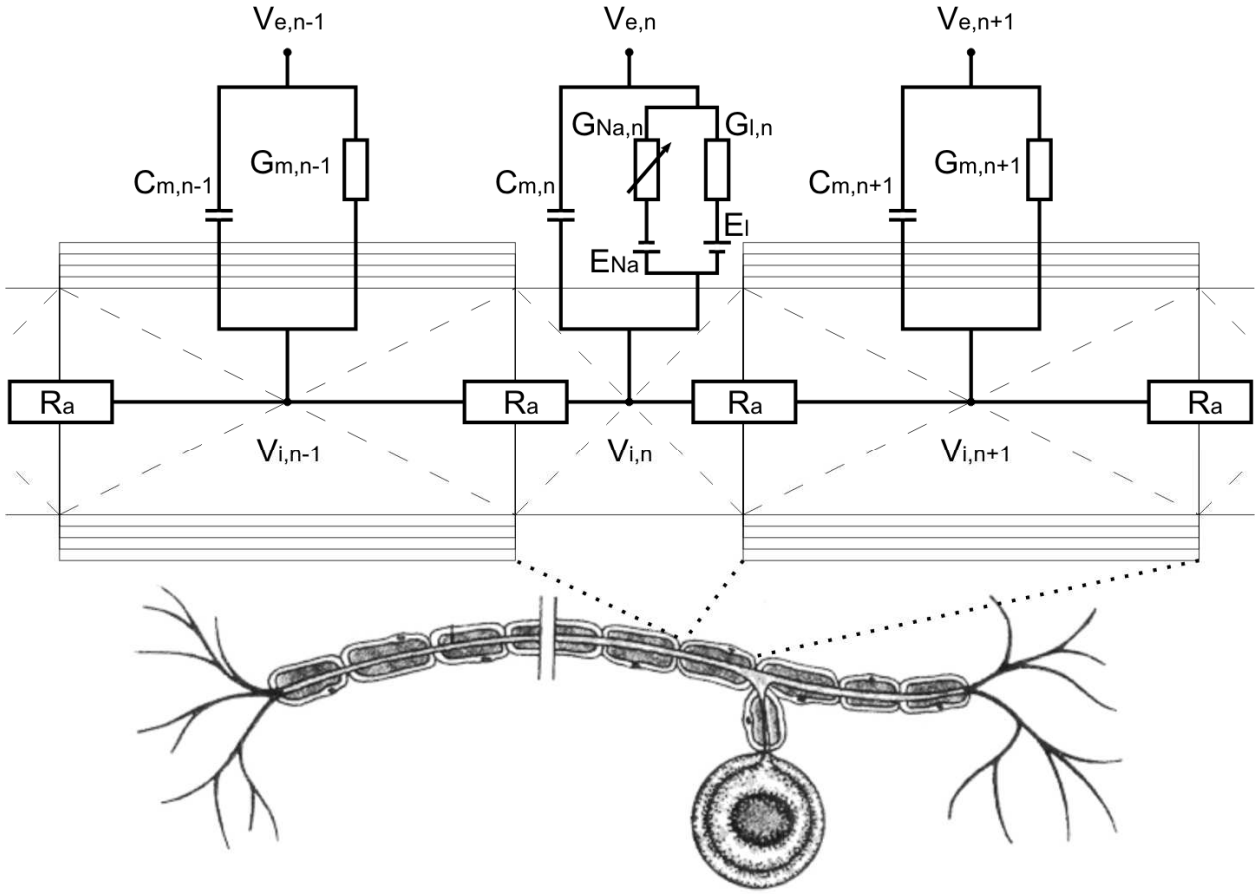

Figure 2.5: The equivalent circuit of the CRRSS model. In contrast to the McNeal model also the myelin is modeled as separate compartments with a conductance and a capacity. The node of Ranvier is modeled with one active ion channel, the Na ion channel (adapted from Ladenbauer et al., 2010).

the compartment diameter d, the length l and the specific membrane capacity c_m or axoplasmatic resistivity ρ. They can be calculated by:

$$c = c_m d \pi l \tag{2.21}$$

$$R_a = \rho \frac{4l}{d^2 \pi}. \tag{2.22}$$

For the internode I^{active} equals 0 and c and g^{lk} are calculated as follows:

$$c = \frac{c_m}{N} d\pi l \tag{2.23}$$

$$g^{lk} = \frac{g_m}{N} d\pi l \tag{2.24}$$

where N is the number of myelin layers.

For the node of Ranvier I^{active} consists of a single sodium channel that is specified by

$$I^{active} = G^{Na} m^2 h (V^m - E^{Na}) \tag{2.25}$$

$$G^{Na} = g^{Na} d\pi l \tag{2.26}$$

where E^{Na} is the sodium reversal potential and m and h are gating variables that are specified by:

$$\frac{dm}{dt} = [\alpha_m(1-m) - \beta_m m]k \tag{2.27}$$

$$= [-(\alpha_m + \beta_m)m + \alpha_m]k \tag{2.28}$$

$$\frac{dh}{dt} = [\alpha_h(1-h) - \beta_h h]k \tag{2.29}$$

$$= [-(\alpha_h + \beta_h)h + \alpha_h]k \tag{2.30}$$

$$k = 3^{0.1T-3.7} \tag{2.31}$$

$$\alpha_m = \frac{97 + 0.363V^m}{1 + \exp(\frac{31-V^m}{5.3})} \tag{2.32}$$

$$\beta = \frac{\alpha_m}{\exp(\frac{V^m-23.8}{4.17})} \tag{2.33}$$

$$\alpha = \frac{\beta_h}{\exp(\frac{V^m-5.5}{5})} \tag{2.34}$$

$$\beta = \frac{15.6}{1 + \exp(\frac{24-V^m}{10})} \tag{2.35}$$

where T is the temperature. All parameters are taken from Ladenbauer (2008) and are listed in table 2.1.

Table 2.1: Parameters of the CRRSS model

Fiber diameter	D	variable
Axon diameter	d	$0.64\dot{D}$ cm
Node length	l_n	$1.5 \cdot 10^{-4}$ cm
Internode length	l_n	$100D$ cm
Specific membrane capacity	c_m	1 µF/cm^2
Axoplasmatic resistivity	ρ	0.07 kΩcm
Membrane conductivity, passive	g_m	1 mS/cm^2
Number of myelin sheath layers	N	$75 \cdot 10^4 D$
Sodium channel conductivity	g^{Na}	1445 mS/cm^2
Leak channel conductivity	g^{lk}	128 mS/cm^2
Equilibrium potential for sodium channels	E^{Na}	115 mV
Equilibrium potential for leakage conductance	E^{lk}	-0.01 mV

Adapted from Ladenbauer (2008)

MRG model

In the following the MRG model is described according to Danner (2010)[1]: The McIntyre-Richardson-Grill (MRG) axon model has as a double-cable structure where current flows both in the axonal and in the the space between the axon and the myelin sheath, the periaxonal space. The model follows the hypothesis that the geometry of the axon plays a major role in its function. With the exception of Halter and Clark (1991) previous models were not strictly based on the morphology obtained from experiments (McIntyre et al., 2002). It was shown that the myelin attachment segment (MYSA) of the axon plays an important role in the depolarizing after potentials (DAP), thus a model should incorporate these parts of the axon (Barrett and Barrett, 1982; McIntyre et al., 2002). According to Barrett and Barrett (1982) the importance of the DAP lies in the increased excitability shortly after an action potential and that the DAP is subject to a passive capacitative current, which is probably a result of a discharge of the internodal axonal membrane capacitance through a resistive

[1]All equations and the derivations of the equations are taken from Danner (2010)

current pathway beneath or through the myelin sheath. Thus, the double cable structure and sophistic modeling of the myelin sheath as well as the myelin attachment and paranodal regions seem plausible and helpful to achieve better results in simulations, at least according to the aforementioned properties. Later, it was shown that the MRG model realistically reproduces excitation threshold values in the case of transcutaneous electrical stimulation (Kuhn, 2008; Kuhn et al., 2009). This phenomenon was subsequently confirmed for the case of transcutaneous and epidural spinal cord stimulation (Danner, 2010). In comparison the CRRSS model has been shown to overestimate the threshold values of extracellular stimulation Wesselink et al. (1999).

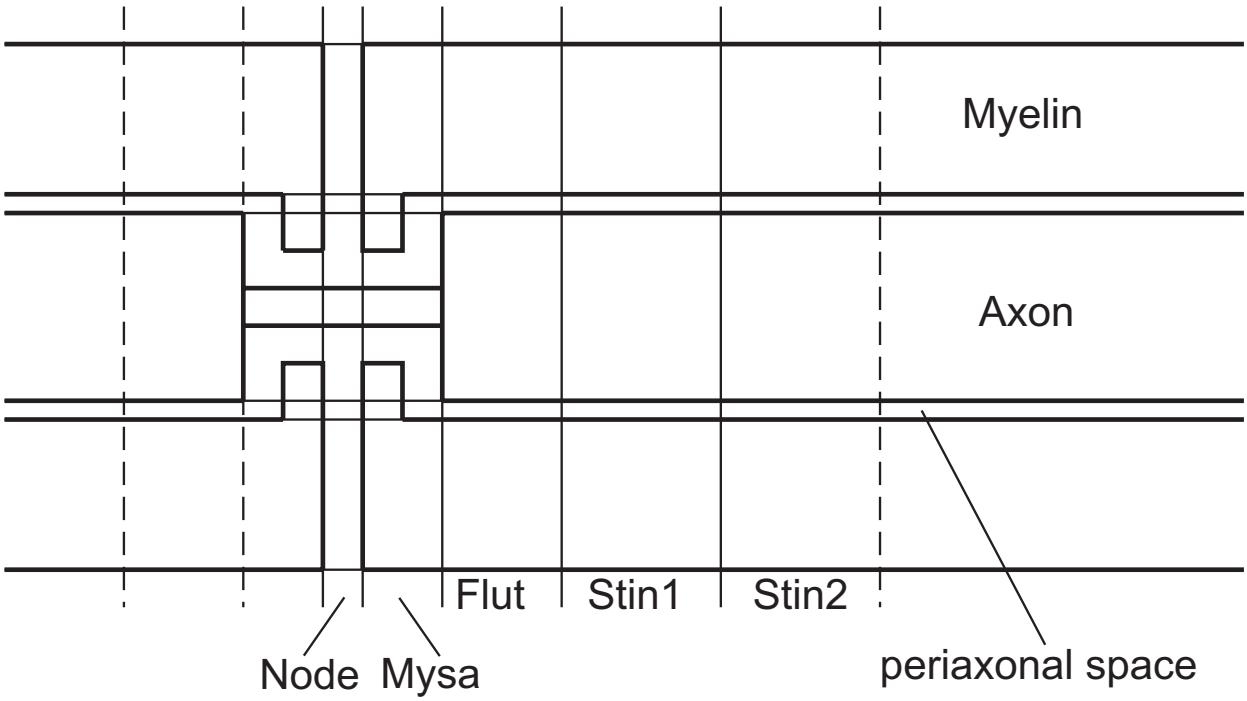

Figure 2.6: Visualisation of the geometry and the compartments of the MRG model (adapted from Danner, 2010).

The geometry of the MRG model consists of 10 segments between two neighboring nodes. Namely the myelin attachment segment (MYSA), the paranode main segment (FLUT) and internode segments (STIN). The abbreviations

Table 2.2: MRG model electrical parameters

Nodal capacitance	c_n	2 μF/cm^2
Internodal capacitance	c_i	2 μF/cm^2
Myelin capacitance	c_m	0.1 μF/cm^2
Axoplasmic resistivity	p_a	70 Ω · cm
Periaxonal resistivity	p_p	70 Ω · cm
Myelin conductance	g_m	0.001 S/cm^2
MYSA conductance	g_a	0.001 S/cm^2
FLUT conductance	g_f	0.0001 S/cm^2
STIN conductance	g_i	0.0001 S/cm^2
Maximum fast Na^+ conductance	g_{Naf}	3.0 S/cm^2
Maximum slow K^+ conductance	g_{Ks}	0.08 S/cm^2
Maximum persistent Na^+ conductance	g_{Nap}	0.01 S/cm^2
Nodal leakage conductance	g_{Lk}	0.007 S/cm^2
Na^+ Nernst potential	E_{Na}	50.0 mV
K^+ Nernst potential	E_K	−90 mV
Leakage reversal potential	E_{Lk}	−90 mV
Rest potential	V_{rest}	−80 mV

stand for *(i)* STIN: stereotyped internodal region *(ii)* FLUT paranodal main segment, because of it being a crenated or fluted region. The detailed geometry is illustrated in figure 2.6. Models for ten different fiber diameters ranging from 2 to 16.0μm (see table 2.3) are supplied. For all other diameters interpolation, and possibly extrapolation, of the parameters can be applied. The Hodgkin and Huxley (1952) like nodal membrane dynamics are modeled for fast (Naf) and persistent (Nap) sodium and slow potassium (Ks). Optional fast potassium (Ks) channels in the paranodal main segment were tested with little effect (McIntyre et al., 2002).

To simulate the model it is divided into compartments. In order to represent the double cable structure, every segment—except the node of Ranvier, which is not surrounded by myelin and therefore has no periaxonal space—consists of two compartments. One in the axonal and one in the periaxonal space. Every

compartment can be described by an equivalent electrical circuit. In figure 2.7 the equivalent electrical circuit of the whole model is illustrated and in table 2.2 the electrical properties are listed.

In the following the equations for non-nodal segments, followed by the equations for the node of Ranvier will be described.

Non-nodal Segments For each segment k two compartments have to be calculated, one for the inner-axonal space (denoted with the superscript i) and one for the periaxonal space (denoted with the superscript p). Note that although the MRG model in contrary to the model of Halter and Clark (1991) does not simulate the outer boundary membrane, such simulations could be useful when the surrounding is spatially restricted or interactions of two or more axons are of interest.

Potentials that are measured against the ground are referred to with the letter E.

$$V_k^i = E_k^i - E_k^p, and \tag{2.36}$$

$$V_k^p = E_k^p - E_k^e \tag{2.37}$$

are the potential differences between inner-axonal / periaxonal and periaxonal / extracellular space respectively. V_k^i can also be referred to as the membrane voltage and is equivalent to V^m for the node of Ranvier. $I_k^{ax,left}$ and $I_k^{ax,right}$ are the currents flowing from the left and right node, respectively. And I_k^{mem} is the current flowing through the membrane. I_k^{mem} consists of a ionic ($I_k^{mem,ion}$) and a capacitive ($I_k^{mem,cap}$) component.

Following the schematics of the the equivalent circuit in Figure 2.7 the equations for the k-th segment are derived (Danner, 2010).

First, the equations for the inner-axonal compartments:

$$I_k^{ax,left} + I_k^{ax,right} + I_k^{mem} = 0 \tag{2.38}$$

where

$$I_k^{ax,left} = \frac{E_k^i - E_{k-1}^i}{\frac{R_k^i + R_{k-1}^i}{2}} \tag{2.39}$$

$$I_k^{ax,right} = \frac{E_k^i - E_{k+1}^i}{\frac{R_k^i + R_{k+1}^i}{2}} \tag{2.40}$$

and

$$I_k^{mem} = I_k^{mem,ion} + I_k^{mem,cap} \tag{2.41}$$

$$I_k^{mem,ion} = G_k^{mem} \cdot (E_k^i - E_k^p - E_k^{pas}) \tag{2.42}$$

$$I_k^{mem,cap} = C_k^{mem} \cdot \frac{d(E_k^i - E_k^p)}{dt} \tag{2.43}$$

now when inserted in the first equation we get

$$\frac{E_k^i - E_{k-1}^i}{\frac{R_k^i + R_{k-1}^i}{2}} + \frac{E_k^i - E_{k+1}^i}{\frac{R_k^i + R_{k+1}^i}{2}} + G_k^{mem} \cdot (E_k^i - E_k^p - E_k^{pas}) + C_k^{mem} \cdot \frac{d(E_k^i - E_k^p)}{dt} = 0 \tag{2.44}$$

and after simplification and substituting V_k^i for $E_k^i - E_k^p$ we get

$$\frac{dV_k^i}{dt} = -\left(G_k^{mem} \cdot (V_k^i - E_k^{pas}) + \frac{E_k^i - E_{k-1}^i}{\frac{R_k^i + R_{k-1}^i}{2}} + \frac{E_k^i - E_{k+1}^i}{\frac{R_k^i + R_{k+1}^i}{2}} \right) / C_k^{mem} \tag{2.45}$$

Next we derive the the equations to calculate the periaxonal compartments:

$$I_k^{px,left} + I_k^{px,right} + I_k^{myelin} - I_k^{mem} = 0 \tag{2.46}$$

$$I_k^{px,left} = \frac{E_k^p - E_{k-1}^p}{\frac{R_k^p + R_{k-1}^p}{2}} \tag{2.47}$$

$$I_k^{px,right} = \frac{E_k^p - E_{k+1}^p}{\frac{R_k^p + R_{k+1}^p}{2}} \tag{2.48}$$

$$I_k^{myelin} = I_k^{myelin,ion} + I_k^{myelin,cap} \tag{2.49}$$

$$I_k^{myelin,ion} = G_k^{myelin} \cdot (E_k^p - E_k^e) \tag{2.50}$$

$$I_k^{myelin,cap} = C_k^{myelin} \cdot \frac{d(E_k^p - E_k^e)}{dt} \tag{2.51}$$

$$I_k^{px,left} + I_k^{px,right} + I^{myelin} + G_k^{mem} \cdot (E_k^i - E_k^p - E_k^{pas}) + C_k^{mem} \cdot \frac{d(E_k^i - E_k^p)}{dt} = 0 \tag{2.52}$$

Now we can substitute $C_k^{mem} \cdot \frac{d(E_k^p - E_k^p)}{dt}$ with (2.45), which results in:

$$I_k^{px,left} + I_k^{px,right} + I_k^{myelin} + I_k^{ax,left} + I_k^{ax,right} = 0 \tag{2.53}$$

and after substituting V_k^p for $E_k^p - E_k^e$

$$\frac{dV_k^p}{dt} = -\left(G_k^{myelin} \cdot V_k^p + \frac{E_k^i - E_{k-1}^i}{\frac{R_k^i + R_{k-1}^i}{2}} + \frac{E_k^i - E_{k+1}^i}{\frac{R_k^i + R_{k+1}^i}{2}} + \frac{E_k^p - E_{k-1}^p}{\frac{R_k^p + R_{k-1}^p}{2}} + \frac{E_k^p - E_{k+1}^p}{\frac{R_k^p + R_{k+1}^p}{2}} \right) / C_k^{myelin} \tag{2.54}$$

The nodal segments are not covered by myelin and thus have no periaxonal space (see Figure 2.7). Therefore the $I^{px,left}$ and $I^{px,right}$ are connected to E_{node}^e for the left and right MYSA segments respectively.

With (2.45), (2.54) and the parameters from tables 2.2 and 2.3 all non-nodal segments can be simulated.

Node of Ranvier As stated before, the node consists of fast and persistent Na^+, slow K^+, a leakage conductance and a capacitance in parallel (see figure 2.7). According to Hodgkin and Huxley (1952) these ionic currents can be written in general form as

$$I_{ion} = g_{ion} \cdot (V - E_{ion}) \tag{2.55}$$

Where g_{ion} consists of the maximum conductance of the ion channels multiplied by a number of gating variables, with a range from 0 to 1. The time dependent differential equations for the gating parameters (γ) is given by

$$\frac{d\gamma}{dt} = \alpha_\gamma \cdot (1 - \gamma) - \beta_\gamma \cdot \gamma \tag{2.56}$$

In the following paragraphs the membrane dynamics for fast and persistent Na^+ (I^{Naf} and I^{Nap} respectively) and the slow K^+ (I^{Ks}) at the temperature of 36 Degrees Celsius are listed.

Fast sodium current

$$I^{Naf} = g_{Naf} \cdot m^3 \cdot h \cdot (V^i - E_{Na}) \tag{2.57}$$

$$\alpha_m = \frac{6.57 \cdot (V^i + 21.4)}{1 - e^{-(V^i+21.4)/10.3}} \tag{2.58}$$

$$\beta_m = \frac{0.304 \cdot (-V^i - 25.7)}{1 - e^{(V^i+25.7)/9.16}} \tag{2.59}$$

$$\alpha_h = \frac{0.34 \cdot (-V^i - 114)}{1 - e^{(V^i+114)/11}} \tag{2.60}$$

$$\beta_h = \frac{12.6}{1 - e^{-(V+31.8)/13.4}} \tag{2.61}$$

Persistent sodium current

$$I^{Nap} = g_{Nap} \cdot p^3 \cdot (V^i - E_{Na}) \tag{2.62}$$

$$\alpha_p = \frac{0.0353 \cdot (V^i + 27)}{1 - e^{-(V^i+27)/10.2}} \tag{2.63}$$

$$\beta_p = \frac{0.000883 \cdot (-V^i - 34)}{1 - e^{(V^i+34)/10}} \tag{2.64}$$

Slow potassium current

$$I^{Ks} = g_{K_s} \cdot s \cdot (V^i - E_k) \tag{2.65}$$

$$\alpha_s = \frac{0.3}{1 - e^{(V^i+53)/-5}} \tag{2.66}$$

$$\beta_s = \frac{0.03}{1 - e^{(V^i+90)/-1}} \tag{2.67}$$

The equations for the node can be derived analogously to Equation 2.45 except that

$$I^{mem} = I^{Naf} + I^{Nap} + I^{Ks} + I^{Lk} + I^{mem,cap} \tag{2.68}$$

where

$$I^{Lk} = G^{mem} \cdot (V^i - E^{Lk}) \tag{2.69}$$

which results in

$$\frac{dV_k^i}{dt} = -\left(I^{Naf} + I^{Nap} + I^{Ks} + I^{Lk} + I^{ax,left} + I^{ax,right}\right)/C_k^{mem} \tag{2.70}$$

Extracellular Stimulation It is possible to calculate the equivalent intracellular current (I^{int}) of an extracellular stimulation. This is done by adding

$$I^{int} = \frac{E_k^e - E_{k+1}^e}{\frac{R_k^i + R_{k+1}^i}{2}} + \frac{E_k^e - E_{k-1}^e}{\frac{R_k^i + R_{k-1}^i}{2}} \tag{2.71}$$

to the to intracellular compartment (Warman, Grill, and Durand, 1992; Grill, 1999). According to Richardson, McIntyre, and Grill (2000) it is sufficient to use the equivalent injected intracellular current only for the the intraxonal compartments and neglect the periaxonal compartments. To adopt the equations we need to substitute E^e with 0 and add I^{int} to the currents in equation 2.45 and 2.70.

Now the final equations used in the simulation are as follows (Danner, 2010):

Interaxonal segments for non-nodal compartments:

$$\frac{dV_k^i}{dt} = -\left(G_k^{mem} \cdot (V_k^i - E_k^{pas}) + \frac{E_k^i - E_{k-1}^i}{\frac{R_k^i + R_{k-1}^i}{2}} + \frac{E_k^i - E_{k+1}^i}{\frac{R_k^i + R_{k+1}^i}{2}} + \frac{E_k^e - E_{k+1}^e}{\frac{R_k^i + R_{k+1}^i}{2}} + \frac{E_k^e - E_{k-1}^e}{\frac{R_k^i + R_{k-1}^i}{2}}\right)/C_k^{mem} \tag{2.72}$$

Periaxonal segments for non-nodal compartments:

$$\frac{dV_k^p}{dt} = -\left(G_k^{myelin} \cdot V_k^p + \frac{E_k^i - E_{k-1}^i}{\frac{R_k^i + R_{k-1}^i}{2}} + \frac{E_k^i - E_{k+1}^i}{\frac{R_k^i + R_{k+1}^i}{2}} + \frac{E_k^p - E_{k-1}^p}{\frac{R_k^p + R_{k-1}^p}{2}} + \frac{E_k^p - E_{k+1}^p}{\frac{R_k^p + R_{k+1}^p}{2}} + \frac{E_k^e - E_{k+1}^e}{\frac{R_k^i + R_{k+1}^i}{2}} + \frac{E_k^e - E_{k-1}^e}{\frac{R_k^i + R_{k-1}^i}{2}}\right)/C_k^{myelin} \tag{2.73}$$

Node:

$$\frac{dV_k^i}{dt} = -\left(I^{Naf} + I^{Nap} + I^{Ks} + I^{Lk} + \frac{E_k^i - E_{k-1}^i}{\frac{R_k^i + R_{k-1}^i}{2}} + \frac{E_k^i - E_{k+1}^i}{\frac{R_k^i + R_{k+1}^i}{2}} + \frac{E_k^e - E_{k+1}^e}{\frac{R_k^i + R_{k+1}^i}{2}} + \frac{E_k^e - E_{k-1}^e}{\frac{R_k^i + R_{k-1}^i}{2}} \right) / C_k^{mem} \tag{2.74}$$

For equation 2.73 $E^p = V^p$ now holds and for the nodal equation (3.18) the membrane voltage V^i is equivalent to E^i. These facts can be exploited to simplify the simulation.

Parameters The absolute conductances, resistances and capacitances used in the equations above can be calculated from the density units in table 2.2 and the geometrical properties from the chosen model in table 2.3.

Let l_k be the length and d_k the diameter of the segment k, then the axonal resistance (R_k^{ax}), the membrane capacity (C_k^{mem}) and the membrane conductance (G_k^{mem}) are

$$R_k^{ax} = \frac{4 \cdot p_a \cdot l}{d^2 \cdot \pi} \tag{2.75}$$

$$C_k^{mem} = c_k \cdot l_k \cdot d_k \cdot \pi \tag{2.76}$$

$$G_k^{mem} = g_k \cdot l_k \cdot d_k \cdot \pi \tag{2.77}$$

In order to calculate the absolute parameters for the myelin conductance (G_k^{my}), the myelin capacity (C_k^{my}) and the periaxonal resistivity (R_k^{px}) the number of myelin lamellas (N) and the space between the membrane and the myelin sheath (sp) is needed (see table 2.3). Then they can be calculated as follows:

$$R_k^{px} = \frac{p_p \cdot l}{(d/2 + 2 \cdot sp)^2 - (d/2)^2} \tag{2.78}$$

$$C_k^{my} = \frac{c_m \cdot d_k \cdot l_k \cdot \pi}{2N} \tag{2.79}$$

$$G_k^{my} = \frac{g_m \cdot d_k \cdot l_k \cdot \pi}{2N} \tag{2.80}$$

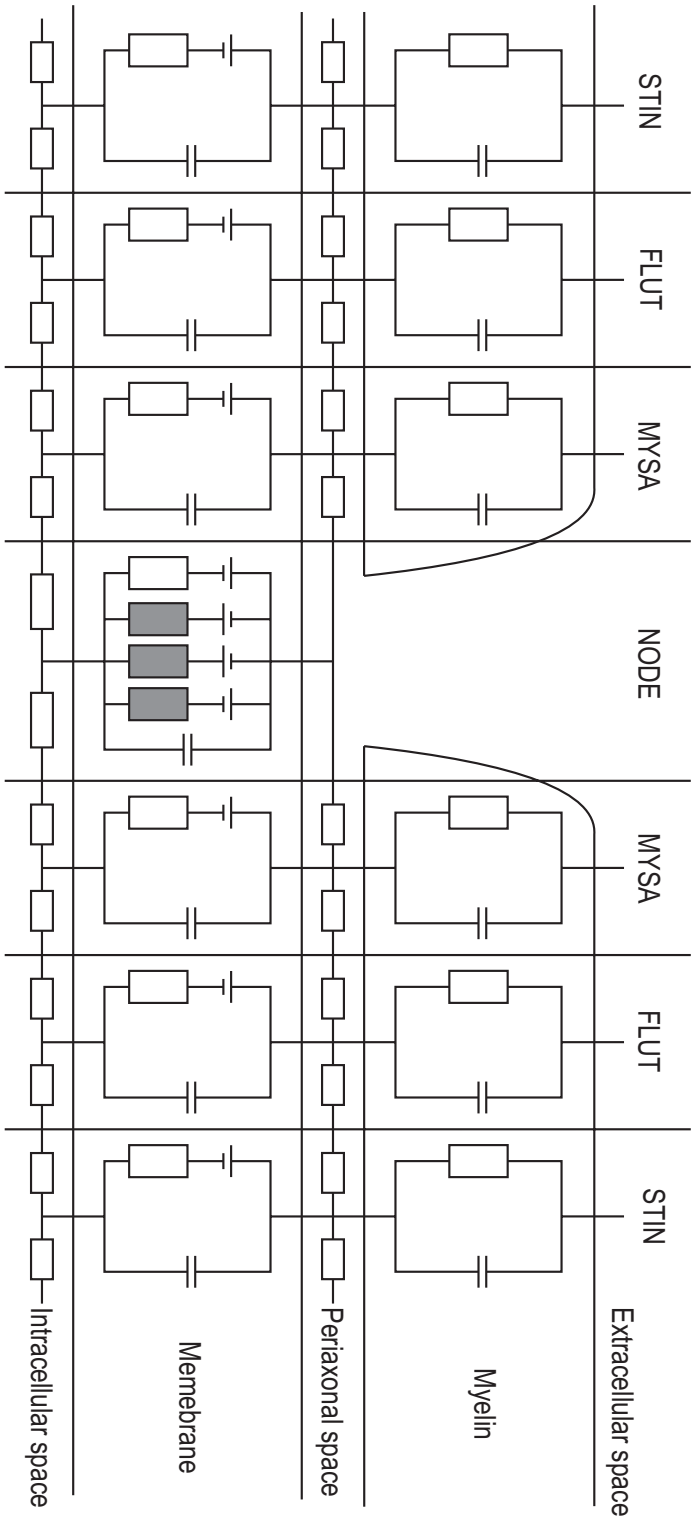

Figure 2.7: Equivalent Circuit for the MRG axon model (adapted from Danner, 2010)

Table 2.3: MRG model geometric parameters

	Fiber Diameter									
	2	5.7	7.3	8.7	10.0	11.5	12.8	14.0	15.0	16.0
Node-node separation	373.2	500	750	1,000	1,150	1,250	1,350	1,400	1,450	1,500
Number of myelin lamella	30	80	100	110	120	130	135	140	145	150
Node length	1	1	1	1	1	1	1	1	1	1
Node diameter	1.4	1.9	2.4	2.8	3.3	3.7	4.2	4.7	5.0	5.5
MYSA length	3	3	3	3	3	3	3	3	3	3
MYSA diameter	1.4	1.9	2.4	2.8	3.3	3.7	4.2	4.7	5.0	5.5
MYSA periaxonal space width	0.002	0.002	0.002	0.002	0.002	0.002	0.002	0.002	0.002	0.002
FLUT length	10	35	38	40	46	50	54	56	58	60
FLUT diameter	1.6	3.4	4.6	5.8	6.9	8.1	9.2	10.4	11.5	12.7
FLUT periaxonal space with	0.004	0.004	0.004	0.004	0.004	0.004	0.004	0.004	0.004	0.004
STIN length	6.2.	70.5	111.2	152.2	175.2	190.5	205.8	213.5	221.2	228.8
STIN diameter	1.6	3.4	4.6	5.8	6.9	8.1	9.2	10.4	11.5	12.7
STIN periaxonal space with	0.004	0.004	0.004	0.004	0.004	0.004	0.004	0.004	0.004	0.004

All values are in μm MYSA, myelin attachment section of paranode; FLUT, main section of paranode; STIN, internodal section, 6 total in 1 internode (McIntyre et al., 2002, 2004).

Chapter 3

The application

In this chapter the application, dubbed *AxonSim*, is described in detail. First, in section 3.1 the details of the implementation are elaborated and a comprehensive manual/documentation is given for users and second, the chapter is concluded with section 3.2, which illustrates a list of examples of stimulation cases.

3.1 Implementation and documentation

To be easy to use and to allow for easy extension and adaption, the application has been written in Matlab 2010b (Mathworks Inc.) with the CVODE differential equation solver from the Suite of nonlinear differential/algebraic equation solvers (SUNDIALS) Version 2.4.0 (Hindmarsh, Brown, Grant, Lee, Serban, Shumaker, and Woodward, 2005). The sundialsTB Matlab bindings, supplied with the SUNDIALS distribution were used to interface the CVODE solver in Matlab. The application, including its source code, is available to download from `http://code.google.com/p/axonsim/`.

Depending on the field of application, different installation options can be chosen when operating with the Suite of solvers. If the full installation of the SUNDIALS distribution is not required, the sundialsTB Matlab binding

can be easily achieved as shortly pointed out in the following. Otherwise one can decide to follow the Cmake-based Installation of SUNDIALS which can be accomplished with the help of cygwin or Visual Studio if Windows is the OS (see `http://sundials.wikidot.com/start` for details).

The sundialsTB is used as a Matlab interface to the SUNDIALS solvers and therefore is part of the whole Suite which has to be downloaded as a first step. After choosing the appropriate sundials-2.4.0.tar file according to the OS, it should be unzipped to a suitable directory, e.g., C:\Sundial or also C:\Programs\Sundial. As a next step open Start - Run and execute cmd to open the command window in order to start the compilation of sundialsTB. Matlab will be launched in sundialsTB by using the commands cd & Matlab including the path to the directory where the SUNDIALS package was unpacked. For example,

```
> cd C:\Programme\Sundials\sundials-2.4.0\sundialsTB
> matlab
```

The Matlab window will open and the install_STB.m file shall be executed. The installation allows to choose the required solvers and also if a toolbox shall be included. In order to do so, different installation folders are possible, which is explained in detail in the readme file located in the \sundialsTB folder. Afterwards the linking of the startup_STB.m file to the original startup.m file of Matlab has to be done according to the chosen configuration (or see `https://computation.llnl.gov/casc/sundials/main.html`).

Alternatively, one can either run the startup_STB.m file from the defined installation directory in order to open Matlab, or also start Matlab and run the startup_STB.m first before experimenting with the AxonSim application which will be examined in the following.

The user interface

The user interface (UI) is designed to summarize all important parameters and plots into one window (see figure 3.1). The program is started by starting Matlab and stepping into the code directory and typing:

```
>> AxonSim
```

This starts the program and displays the user interface (figure 3.1). When initiated already some parameters are set and the simulation can be started. Pressing *Calculate* starts the simulation according to the set parameters. When *Calculate threshold* is selected the activation threshold, i.e. the minimal stimulation strength needed to elicit an action potential, is calculated using binary search with the set accuracy, otherwise the simulation is performed with the supplied stimulation strength.

In the following all parameters are described in detail:

Electrode This parameter is used to set the type of electrode. There are four types of electrodes:

- **single** This is a single point electrode located in the extracellular space.
- **double** Two point electrodes with an electrode separation set by *Electrode separation* where one electrode uses the same and the other the opposite sign of the *Stimulation strength*.
- **triple** Similar to the former two electrode types, here three point electrodes are created. The middle one uses the *Stimulation strength* as set, the other electrodes use a *Stimulation strength* multiplied by -0.5. All electrodes are separated by *Electrode separation* and are in one line, parallel to a straight fiber.
- **intracellular** In contrary to all aforementioned electrode types, which are all variations of extracellular stimulation, this electrode stimulates using an injected current into a node of Ranvier.

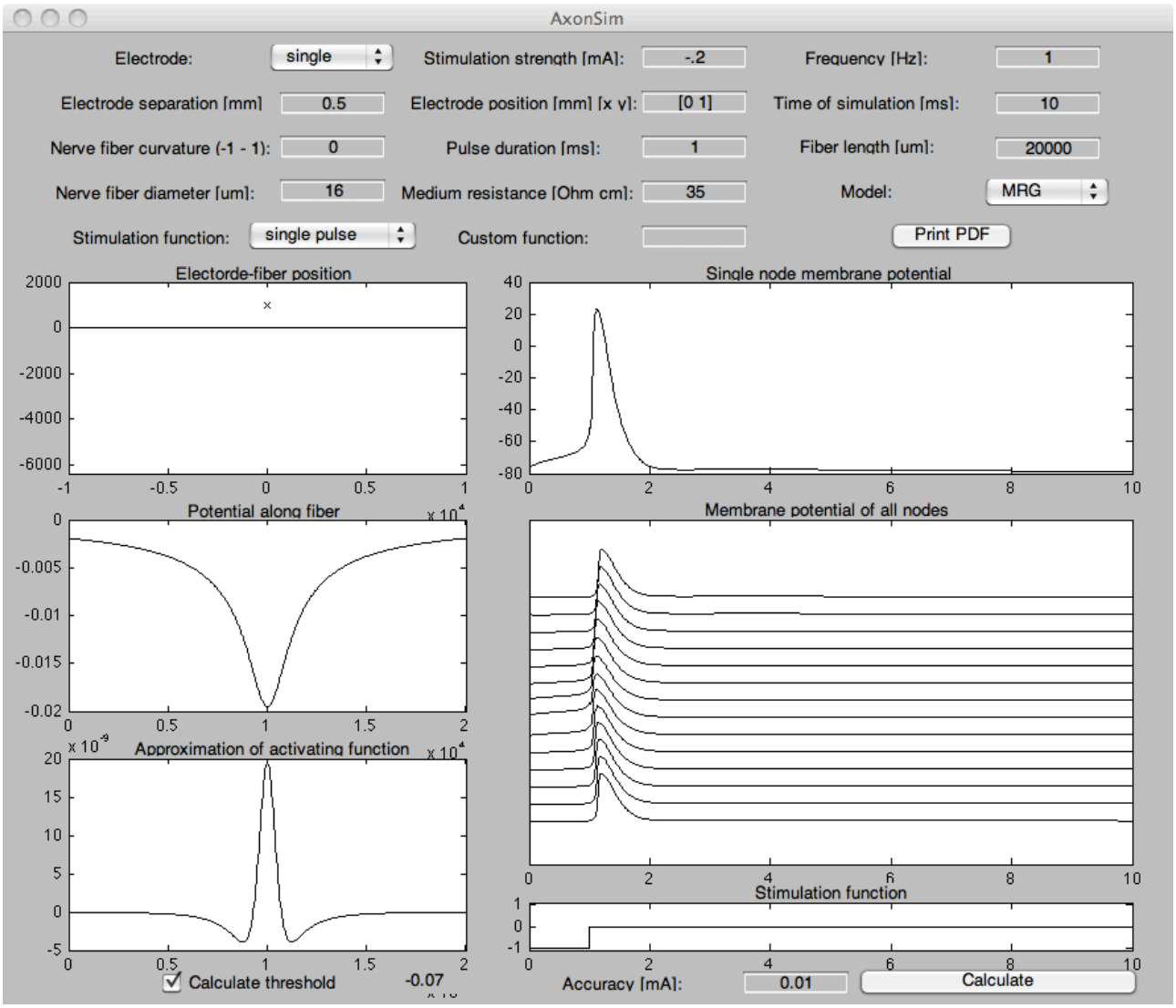

Figure 3.1: The user interface of the application AxonSim. A list of stimulation parameters can be set. The output is displayed in a number of plots. The relative position between the electrode and the fiber is illustrated, followed by the potential distribution, generated by the stimulation electrode and evaluated along the fiber. An approximation of the activating function, i.e. the second order spatial differential, is given, followed by an illustration of the membrane potential of one and all nodes and the stimulation function. Here the result of the binary search with the accuracy of of 0.01 mA to determine the activation threshold of a 20 mm long fiber is shown, thus the illustrated curves represent the result of the stimulation at the activation threshold (-0.07 mA).

Stimulation strength The stimulation strength identifies how much current an electrode generates (please refer to *Electrode* for details on the electrode types). Note that the unit is mA for the extracellular stimulation case and pA for the intracellular stimulation case.

Frequency Describes the frequency, how often the stimulation pulse or in general the stimulation function should be repeated. The frequency is specified in Hz.

Electrode separation This parameter describes the distance between the electrodes if *Electrode* is set to double or triple. Otherwise this setting has no effect.

Electrode position Here the position of the electrode can be specified. This is done by supplying a two dimensional vector to the field in the form of `[x y]` or `[x, y]`, i.e. the usual Matlab style, where x and y are the x- and y-coordinates of the electrode position in mm. In the case of double or triple electrode configurations the coordinates specify the center of the electrodes. In the case of intracellular stimulation the field's name is *Location of electrode (Node)* and the value specifies the node where the current is injected. The value has to be a positive integer and must not be bigger than the maximum number of nodes in the fiber.

Location of electrode (Node) see *Electrode position*

Time of simulation This parameter specifies for how long the simulation should be run. The value is specified in ms. Note that all plots are adjusted to show the whole simulation time.

Nerve fiber curvature This setting lets the user change the curvature of the nerve fiber, the value can be in the interval $[-1, 1]$. 0 denotes a straight fiber, positive values denote curvatures in direction to and negative values

in direction from the stimulating electrode (if *Electrode position* is set as default). 1 and −1 create a half circle out of the fiber. The method how this curvature is generate is described in detail in section 3.1.

Pulse duration This parameter specifies the duration of the stimulation pulses. It only applies to the single and double pulse settings of *Stimulation function*. If a custom stimulation function is chosen this setting has no effect.

Fiber length With this parameter the length of the fiber can be chosen in µm. Note that, especially for the MRG model, an increase in fiber length strongly increases the time needed to compute the solution. The center of the fiber is always at (0,0) and the fiber is extended along the x-axis in both directions.

Nerve fiber diameter With this setting the diameter of the nerve fiber can be chosen. For the MRG model the supplied parameters are used if the diameter matches a diameter with a supplied parameter set, if not the values are interpolated between two parameter sets. For values bigger than 16 µm the parameter values are extrapolated, for values smaller 2 µm the values are linearly scaled. The fiber diameter has to be specified in µm.

Medium resistance Here the specific resistance for the medium in which the fiber and the electrode reside can be specified. For the intracellular stimulation case this setting has no effect. The unit of the resistance is Ω·cm.

Model With this parameter the axon model that will be used for the simulation can be selected. Candidates are the McIntyre-Richards-Grill (MRG; McIntyre et al., 2002) and the Chiu-Ritchie-Rogart-Stagg-Sweeney (CRRSS; Chiu et al., 1979; Sweeney et al., 1987) model.

Stimulation function Here the time dependent function of the stimulation electrode can be set. A single pulse generates a rectangular stimula-

tion pulse with the stimulation strength and sign specified in *Stimulation strength* and duration specified in *Pulse duration*. The double pulse option creates two adjacent rectangular pulses with the same strength and duration, also as specified in *Stimulation strength* and *Pulse duration* but the first pulse has the same sign as specified in *Stimulation strength* and the second pulse is multiplied by -1. The third option, custom, uses a custom stimulation function as specified in *Custom function*.

Custom function In this field a time dependent function can be specified that afterwards is used as the stimulation function. It is only used if *Stimulation function* is set to custom, otherwise it has no effect. The function must fit into one line and can make use of `t`, the time in ms. The output of the function is multiplied with the stimulation strength as specified in *Stimulation strength* or as set by the binary search algorithm to determine the activation threshold. An easy example is to set the custom function to `t` and *Frequency* to 1000 Hz to create a sawtooth wave, with an upper bound of 1 and a lower bound of 0. Note that adjusting the frequency results in a repetition of the function and thus after the reciprocal of the frequency the time `t` is reset to 0. It is also possible to create a custom method and pass it to *Custom function*. For this a Matlab m-file in the directory of the program has to be created that specifies a function that takes up to one argument, the time `t`, and returns a single real value. For examples please refer to section 3.2.

Print PDF When this button is clicked a PDF containing all parameters and plots of the previous simulation is created in the current directory.

Calculate threshold This checkbox can be checked if it is desired to calculate the activation threshold using binary search with the accuracy as specified in *Accuracy*. When checked the *Stimulation strength* is ignored, only the sign of *Stimulation strength* is used. The binary search algorithm

starts with *Accuracy* multiplied by the sign of *Stimulation strength*. The result of the binary search, i.e. the activation threshold, is printed right of the checkbox and the simulation is performed and plotted with the stimulation strength set to the activation threshold. If the box is not checked, the simulation is performed as specified by all other parameters.

Accuracy This parameter determines the accuracy of the binary search algorithm. If *Calculate threshold* is not checked, this field has no effect.

Calculate If calculate is clicked the program simulates the selected nerve fiber model according to the specified parameters and plots the results.

When the simulation is finished a series of plots are drawn, in the following list these plots are described in detail:

Electrode-fiber position In this plot the fiber is drawn as a blue continuous line and the electrode position is marked as one to three x-es, depending on the electrode type. The purpose of this plot is to provide relative geometrical information about fiber and electrode position. Also the fiber curvature can be seen. The units used are µm.

Potential along fiber Here the potential distribution, generated by the extracellularly located electrodes along the fiber is displayed. This is done by calculating the electrical field that is generated by the electrode(s) and evaluating it along the fiber trajectory. The field is calculated using *Stimulation strength* as the current generated by the electrodes, even if a custom stimulation function is used. For custom stimulation functions the generated field is multiplied by the stimulation function and then used as the input for the nerve fiber model as the extracellular voltage. The units displayed are in V for the y-axis and in µm for the x-axis.

Approximation of activating function Here an approximation of the activating function is displayed. This approximation is calculated simply

as the second order spatial difference of the extracellular potential along the fiber. The potential along the fiber is calculated using *Stimulation strength* even when a custom stimulation function is used. As described above the activating function f is proportional to the second order spatial derivate of the potential distribution. Thus, in the discrete case, f_n is proportional to the second order spatial difference of the potential distribution.

Single node membrane potential In this plot the membrane potential V^m of the n-th node is displayed. As a default the 7th node is displayed. Note that for the node of Ranvier V^i as used by the MRG model is equivalent to V^m. The x-axis represents the time and is in ms units and the y-axis is in mV.

Membrane potentials of all nodes Here the membrane potentials V^m of all nodes are displayed. The uppermost line is the leftmost and the lowermost line is the rightmost node of Ranvier in the *Electrode-fiber position* plot. In this plot the propagation and conduction of the action potential can be seen. The x-axis represents the time and is in ms units.

Stimulation function Here the stimulation function, whether a predefined or a custom function, is displayed. The x-axis represents the time and is in ms units and the y-axis represents the the factor k the *Stimulation strength* is multiplied with, at a certain time, due to the stimulation function.

In order to be able to start AxonSim one needs a Matlab version that is compatible with SundialsTB and SundialsTB installed. SundialsTB is part of the standard SUNDIALS package and can be found on SUNDIALS homepage (link: `https://computation.llnl.gov/casc/sundials/main.html`).

Implementation remarks

In this section some remarks are give on how certain features are implemented.

Nerve fiber curvature

The curvature of the nerve fiber is calculated depending on the parameter c that is taken from the parameter *Nerve fiber curvature*. c can be any real number between -1 and 1. If bigger absolute values are chosen, the absolute value is set to 1 while remaining the sign. In the following, only the positive case is treated, to derive the curvature for a negative value of c the curve can be mirrored along the x-axis. If c is 1 the curve is defined as a semicircle with the middle of the line being at x=y=0. And if c equals 0 a straight line should be drawn. For $c = 1$ the radius r can be defined as

$$r = l/\pi \tag{3.1}$$

where l is the length of the fiber. To calculate the values in between $1/c$ is introduced as a factor, resulting in

$$r = 1/c \cdot l/\pi \tag{3.2}$$

or

$$r = \frac{l}{c \cdot \pi}. \tag{3.3}$$

Then the angle α of the circle that comprises the nerve fiber trajectory has to be calculated so that the fiber retains it length l as specified. α is calculated by

$$\alpha = l/r. \tag{3.4}$$

Then x coordinates of points of the fiber trajectory can be calculated as being between $-\sin(\alpha/2)$ and $\sin(\alpha/2)$. Here this is done by setting the first point as $-\sin(\alpha/2)$ and adding l/n, where n is the number of segments, until $x = \sin(\alpha/2)$. The y-coordinate is then calculated by

$$y = -\sqrt{r^2 - x^2} + r. \tag{3.5}$$

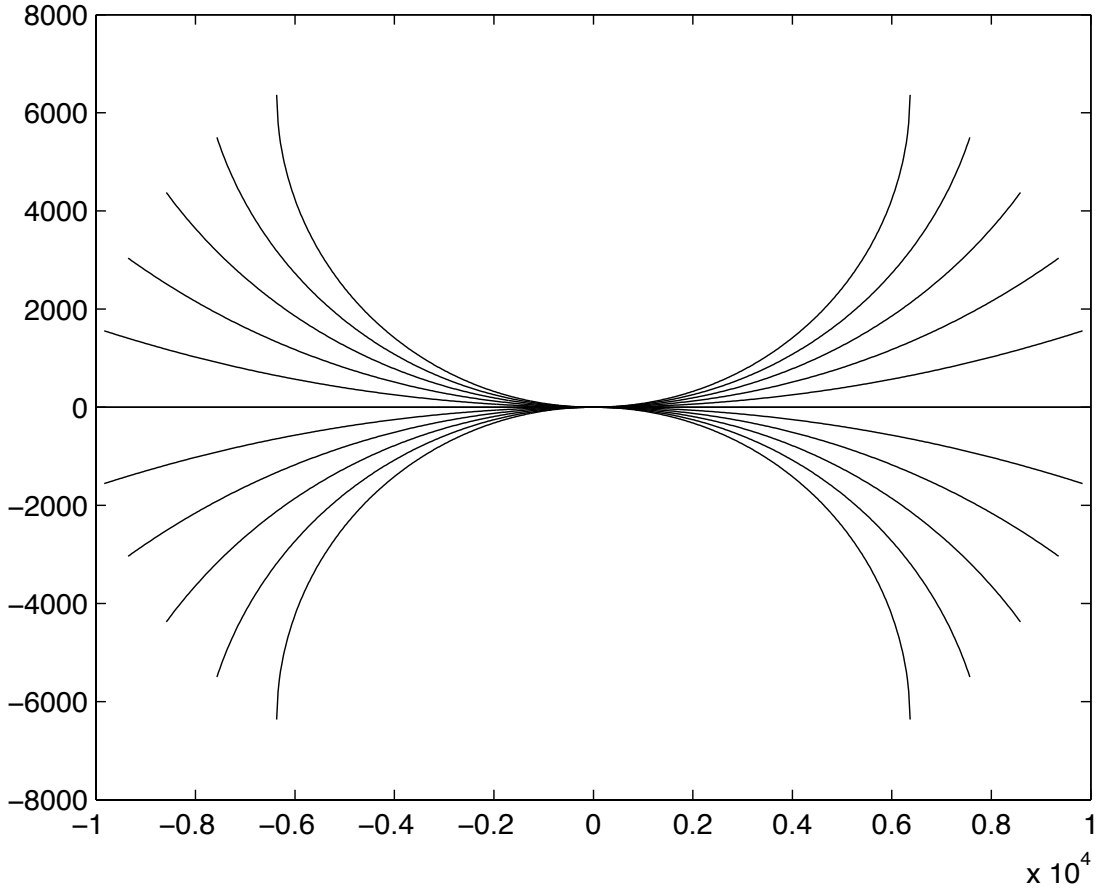

Figure 3.2: Illustration of the results of the function `curvature` for a fiber with the length of 20,000 μm and c values of -1, -0.8, -0.6, -0.4, -0.2, 0, 0.2, 0.4, 0.6, 0.8 and 1. Note that for all negative c values the line is bent in negative y-direction and for positive c values in the positive y-direction. All values are displayed in μm.

The results for 11 values of c between -1 and 1 are illustrated in figure 3.2. And the source code of the function used in the application can be seen in listing 3.1.

Listing 3.1: Method `curvature` to calculate curved trajectories of the fiber. c can be between -1 and 1.

```
function [ x,y ] = curvature( c, length )
    parts=499;
    s = sign(c);
    c=s*c;
    if c > 1
        c=1;
    end
    if c ≠ 0

    r = 1/c*length/pi;
    U = 2*r*pi;
    angle = length/U*2*pi;
    dev=sin(angle/2)*r;
    x = -dev:(2*dev/parts):dev;
    y = -sqrt(r^2 - x.^2);
    y = y+r;
    end
    if c == 0
        x = -length/2:length/parts:length/2;
        y = zeros(1,parts+1);
    end
    y = s.*y;
end
```

Electrical field

For a single point electrode in an infinite homogeneous medium the potential field can be calculated for a point at (x,y), when the electrode is at (0,0) as

follows (note that the z-coordinate is ignored, since here we assume that the electrodes and fibers reside on the xy-plane):

$$V^e = \frac{\rho I_{el}}{4\pi} \cdot \sqrt{x^2 + y^2} \tag{3.6}$$

where V^e is the (extracellular) potential at (x,y), ρ is the specific resistance of the medium and I_{el} is the current of the electrode. Since $\sqrt{x^2 + y^2}$ is the distance d_{el} of the point electrode to the point where the field is evaluated the formula can be written as:

$$V^e = \frac{\rho I_{el}}{4\pi} \cdot d_{el} \tag{3.7}$$

and for N point electrodes:

$$V^e = \sum_{i=1}^{N} \left(\frac{\rho I_{el,i}}{4\pi} \cdot d_{el,i} \right) \tag{3.8}$$

where $I_{el,i}$ is the current of and $d_{el,i}$ the distance from the i-th point electrode. The code used in AxonSim is listed in listing 3.2 and an example of a potential distribution generated by a single and a double electrode along a straight fiber is illustrated in figure 3.3.

Listing 3.2: Method `electrode` to calculate the potential at a point in the xy-plane.

```
function V = electrode(rho,I,xe,ye,x,y )
    q = rho * I;
    d = sqrt((xe-x).^2+(ye-y).^2);
    V = q./(4.*pi.*d);
end
```

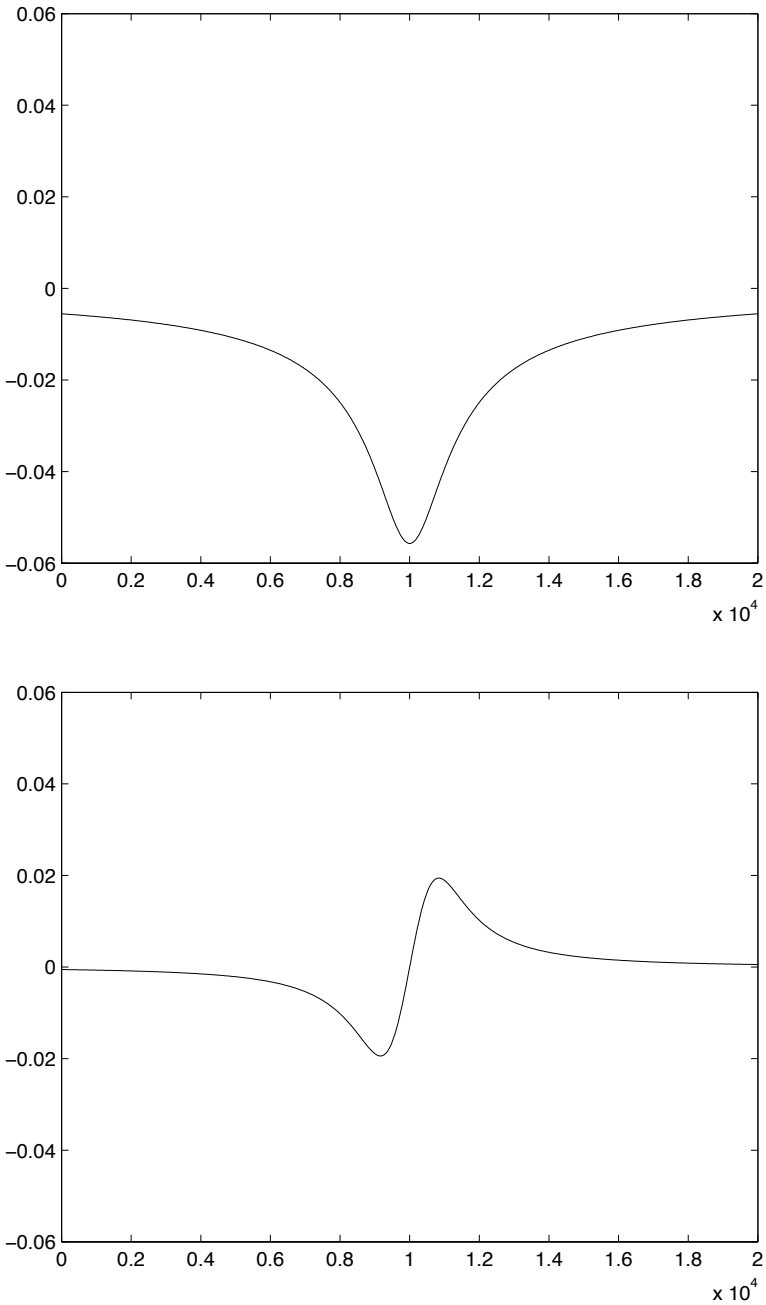

Figure 3.3: Potential distributions evaluated along a straight fiber 20 mm long fiber. The electrodes are located at the middle in a 1 mm distance. Top: single point electrode at -.2 mA. Bottom: two point electrodes, separated by 1 mm, left at -.2 mA and right at .2 mA. Units are in μm and mA for the x- and y-axis, respectively.

Approximation of the activating function

As described in section 2.3, the activating function f is proportional to the second order spatial derivate of the potential distribution along the fiber:

$$f = \frac{d}{4\rho_i c} \cdot \frac{\delta^2 V^e}{\delta x^2}. \tag{3.9}$$

Similarly, the discrete activating function f_n is proportional to the second order spatial difference of the potential distribution along the fiber:

$$f_n = \frac{d\Delta x}{4\rho_i Lc} \frac{V^e_{n-1} - 2V^e_n + V^e_{n+1}}{\Delta x^2}. \tag{3.10}$$

Thus, if $(d\Delta x)/(4\rho_i Lc)$ is substituted by constant factor, e.g. 1, a fiber independent approximation of the activating function is achieved:

$$f_n = \frac{V^e_{n-1} - 2V^e_n + V^e_{n+1}}{\Delta x^2}. \tag{3.11}$$

This is the function that is displayed in the application.

Stimulation functions

As described in section 3.1 there exist two hardcoded stimulation functions, a single pulse and double pulse, both with variable pulse duration and intensity. Further, also custom stimulation functions can be defined, by passing them into the field *Custom function* and setting *Stimulation function* to custom. This function f has to be defined as a function that takes only `t`, the time in ms, as an argument and returns a scalar:

$$f : \mathbb{R} \to \mathbb{R} \tag{3.12}$$

and has to be defined in Matlab code. All variables and functions that are available in the working space can be used. The field calculated and evaluated along the fiber will be multiplied by the result of the function at the time t. Thus, if the function returns 1, the stimulation intensity is as specified in

the parameters. A simple example would be `sin(2*pi*t)/2`. This creates a sinusoid function with the phase of 1 ms and a peak-to-peak amplitude as specified in the parameters.

Only one-line functions can be specified, but since all variables and methods that are available to the workspace are also available here, a custom method can be specified in an m-file and used as a custom stimulation function. Thus, all functions that are realizable in Matlab can be created and used as stimulation functions. In section 3.2 examples using different stimulation functions, including custom m-files, are given.

Binary search

Binary search is a search algorithm that finds an element in the worst case runtime of

$$O(N) = log_2 N \tag{3.13}$$

where N is the number of values in the search space. In our case the search space are the natural numbers and here the worst case runtime is

$$O(N) = 2 \cdot \lceil log_2 k \rceil \tag{3.14}$$

with k being the number to be search. This only applies if the search is performed in $\mathbb{N}$ or $\mathbb{Z}$, if the search is performed in $\mathbb{R}$ the search space has to be discretized. Here this is done by limiting the accuracy to a certain value and thus the search is stopped when the result falls between two values with a maximum distance from each other that is not bigger than the specified accuracy. Thus the activation threshold is defined as the minimal strength, as a multiple of the accuracy, needed to evoke an action potential in a fiber. Thus here k times the accuracy is the activation threshold.

The algorithm works starting with a small value (set using the Accuracy) that should be lower than the activation threshold, then the value is doubled if it is still below the activation threshold. If the value is above the activation

threshold the space between the last sub- and superthreshold values is split in half for as long as the stepsize is smaller than the activation threshold. For an exact algorithm please refer to listing 3.3.

Listing 3.3: The binary search algorithm to find the threshold values (adapted from Danner 2010)

```
step = 1
x = 1
result = 0
grow = 1

while 1
   if model(x) == 1
        grow = 0
        result = x
        x = x - step
        step = step/2
   else
        x = x + step
        if grow == 1
            step = step*2
        else
            step = step/2
        end
   end
   if step < smallestStepSize
       break
   end
end
```

ODE solver

The CVODE solver solves ordinary differential equation initial value problems in real N-space. A usual problem is defined as

$$\frac{dy}{dt} = f(t, y) \tag{3.15}$$

$$y(t_0) = y_0 \tag{3.16}$$

where t is the independent variable, usually the time, y is a N dimensional real vector and f is an arbitrary function. The solver uses variable-order, variable-step multistep methods, which are based on

$$\sum_{i=0}^{K_1} \alpha_{n,i} y_{n-i} + h_n \sum_{i=0}^{K_2} \beta_{n,i} \frac{dy_{n-1}}{dt} = 0 \tag{3.17}$$

where y_n are the computed approximations of $y(t_n)$ and h_n is the step size $t_n - t_{n-1}$. Since here stiff differential equations are solved, (differential equations are called stiff if "one rapidly damped mode, whose time constant is small compared to the time scale of the solution itself" is present; Hindmarsh et al., 2005), backward differentiation formulas (BDFs) in fixed-leading coefficient form are used. These are given by inserting $K_1 = q$ and $K_2 = 0$ into (3.17), where q is variable between 1 and 5. To solve each step, here *Newton iteration* was applied.

3.2 Examples

In this section many properties of the nerve fiber models will be illustrated using AxonSim. Several examples are presented that shall explain how to use the application and simultaneously show how nerve fibers react to certain stimulation properties.

Propagation of an action potential

Usually an action potential is initiated at a single node of Ranvier, the influx of current and the change of the membrane potential at this node influences also neighboring parts of the axon. In the case of the myelinated axons, this influence is transferred to the next node of Ranvier, where the membrane potential is lifted above the threshold level and the active ion channels produce an action potential, subsequently also an action potential is initiated at its neighboring nodes of Ranvier. The propagation of an action potential is always in one direction, since after the initiation of the action potential this node becomes unexcitable for a short period of time but when an action potential is initiated artificially there is no previous node of Ranvier that has been excited and is in an unexcitable state. Thus, when artificial stimulation is used action potentials travel, propagate in all direction away from the initiation site.

Note that each subsequently elicited action potential is subject to a short delay, this results in a finite propagation velocity of the nerve fiber. Depending on the fiber diameter the velocity of action potential conduction ranges from 1 to 100 m/s.

In figure 3.4 an example is shown that uses a point electrode localized 1 mm above the middle of an 20 cm long axon with 16 μm diameter. The electrode stimulates the axon with a current of $I = -0.08$ mA and a single pulse of 1 ms duration. The model used is the MRG model. For all other parameters please refer to the figure.

Intracellular- and extracellular stimulation

With intracellular stimulation an electrode is stuck into the axon itself and current is injected into the intraaxonal space. In mathematical terms, this

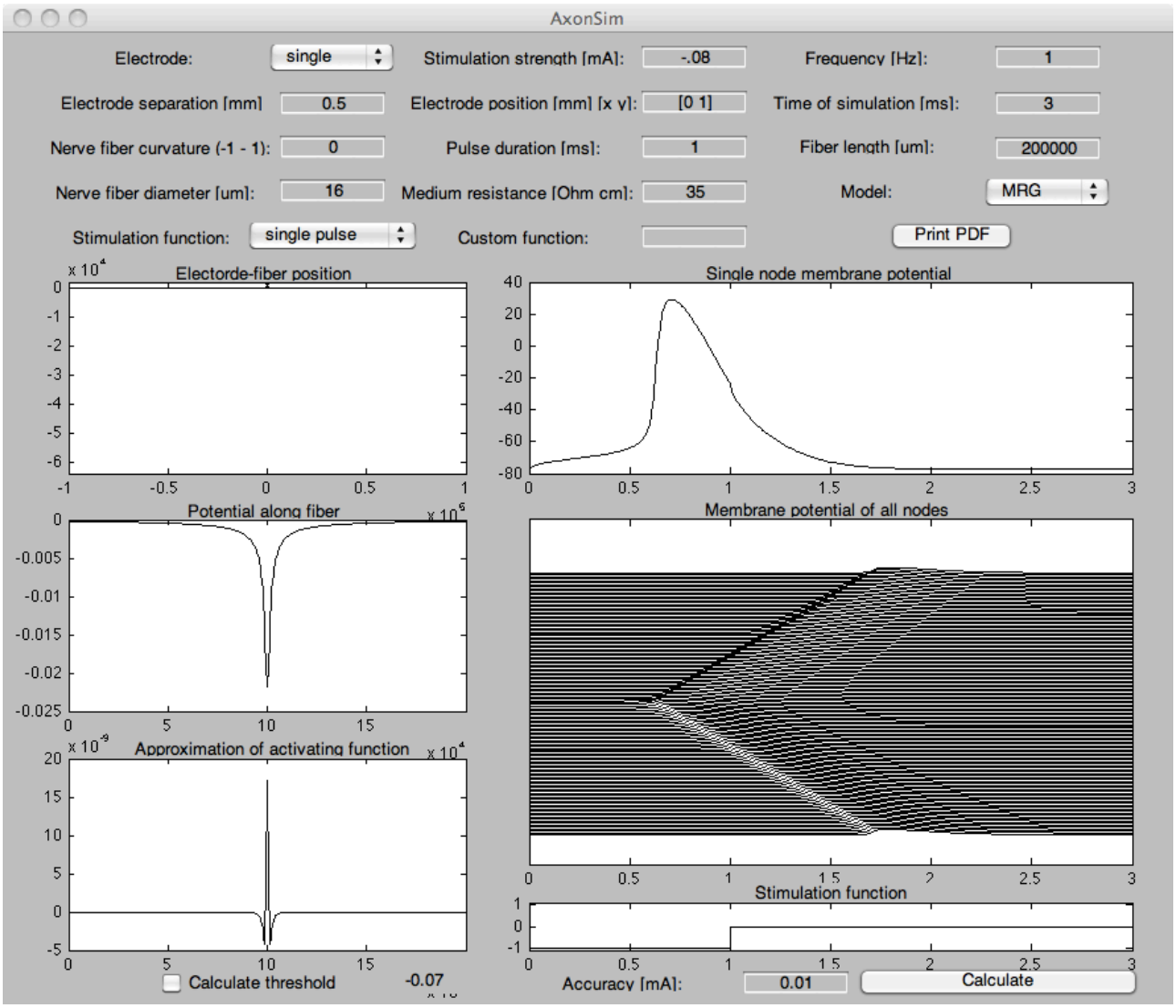

Figure 3.4: Example of an action potential propagation along a 20 cm long nerve fiber. In the plot *Membrane potential of all nodes* the bidirectional propagation of the action potential along the nerve fiber can be seen.

means that (3.18) for the node of Ranvier is adapted as follows:

$$\frac{dV_k^i}{dt} = -\left(I^{Naf} + I^{Nap} + I^{Ks} + I^{Lk} + I^{intstim} + \frac{E_k^i - E_{k-1}^i}{\frac{R_k^i + R_{k-1}^i}{2}} + \frac{E_k^i - E_{k+1}^i}{\frac{R_k^i + R_{k+1}^i}{2}} \right) / C_k^{mem} \tag{3.18}$$

where $I^{intstim}$ is the intracellularly inject stimulation current and the equivalent injected extracellular current I^{inj}

$$I^{inj} = \frac{V_k^e - V_{k-1}^e}{\frac{R_k^i + R_{k-1}^i}{2}} + \frac{V_k^e - V_{k+1}^e}{\frac{R_k^i + R_{k+1}^i}{2}} \tag{3.19}$$

has been removed since the simulation only relies on intracellular stimulation. If a simulation with both, intracellular and extracellular stimulation, is desired, I^{inj} can be added back into the equation.

For intracellular stimulation small fiber diameters have lower thresholds than large fiber diameters (for more information please see section 3.2).

The CRRSS and the MRG model

The CRRSS and the MRG model have several differences. The most important difference for the electrical stimulation of the nervous system is that the MRG model has been reported to realistically reproduce the activation threshold with transcutaneous electrical stimulation (Kuhn et al., 2009), while Wesselink et al. (1999) reported that the CRRSS model overestimates excitation thresholds for extracellularly stimulated myelinated nerve fibers. For the case of spinal cord stimulation this discrepancy in activation threshold values has been confirmed (Danner, 2010). Since AxonSim is able to simulate both axon models, features of both models can be compared.

Figure 3.6 shows the simulation of the CRRSS model under the same conditions as the MRG model in figure 3.1. Differences can be seen in the shape of

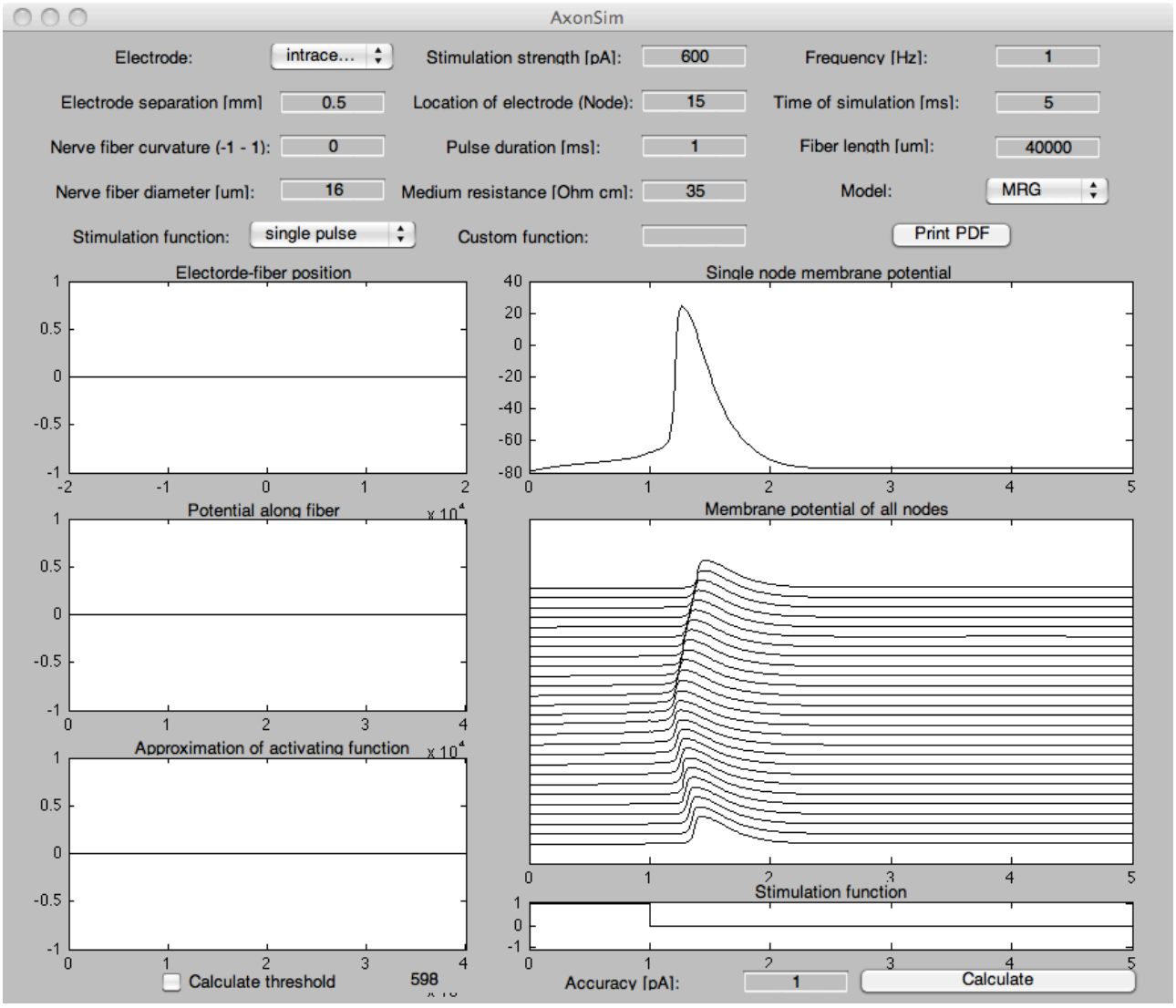

Figure 3.5: Example of intracellular stimulation of 16 µm nerve fiber with 600 pA injected current into the 15-th node with a 1 ms long stimulation pulse. Note that all plots at the left side are empty, since the current is directly injected into a node of Ranvier and no extracellular field acts on the fiber.

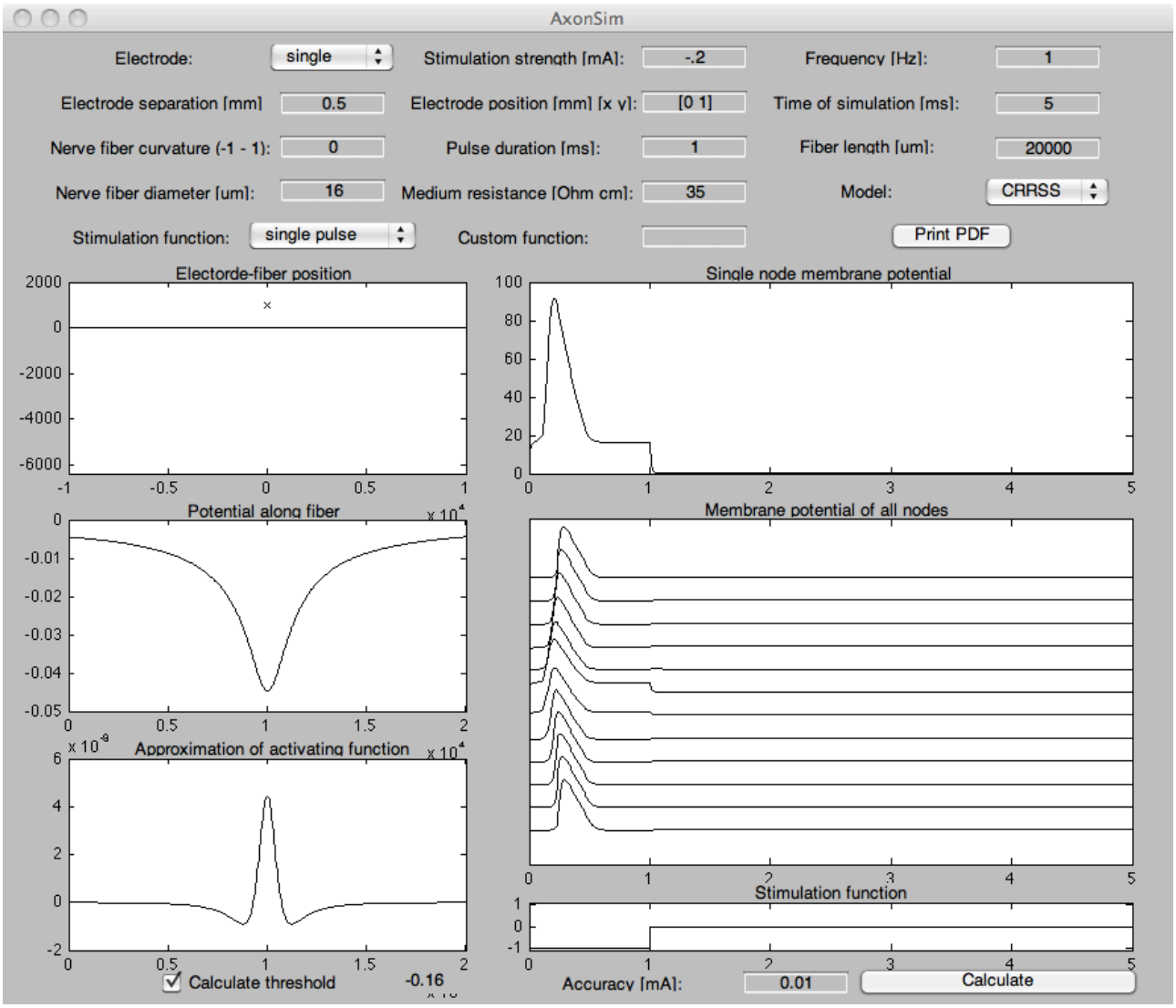

Figure 3.6: Simulation of the CRRSS model with same settings as in figure 3.1. Note that for the CRRSS model the reduced membrane potential is used, where the resting potential is shifted to 0.

the action potential, i.e. with the MRG model the depolarizing after potential is visible. Furthermore, the threshold value of the MRG model is lower than of the CRRSS model, i.e. -0.07 vs. -0.16.

Activation threshold and fiber diameter

The fiber threshold has a big influence on the activation threshold Ranck (1975). It can be differentiated between two different cases:

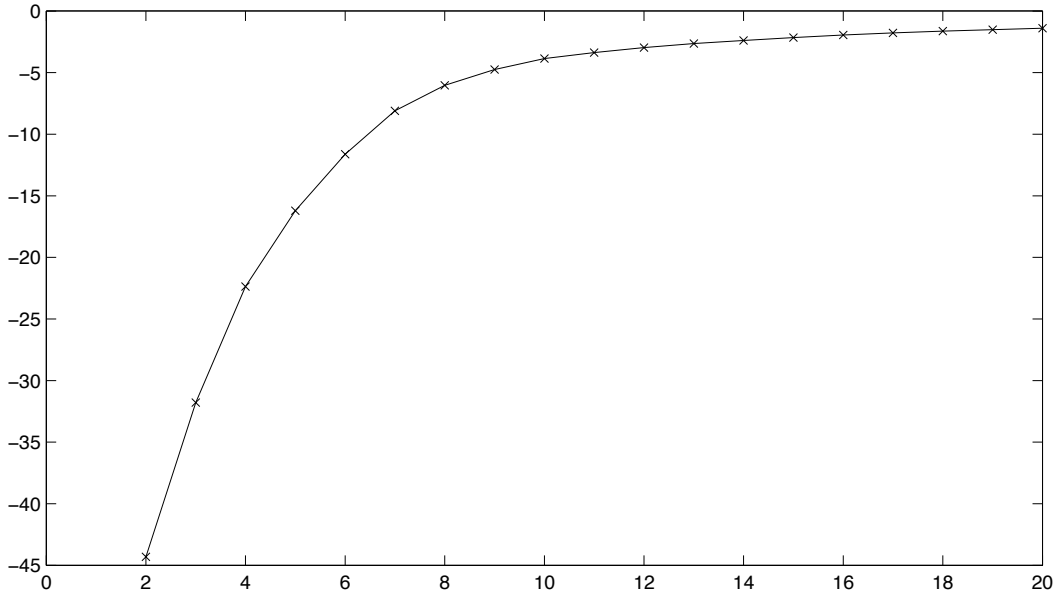

Figure 3.7: Influence of the fiber diameter on the activation threshold for extracellular stimulation. X-axis: fiber diameter in µm, y-axis: activation threshold in mA. The activation threshold decreases with an increasing fiber diameter. Note that the relationship is not linear, an approximately the threshold is proportional to reciprocal of the fiber diameter.

Extracellular stimulation With extracellular stimulation lower thresholds can be achieved with bigger axon diameters. Figure 3.7 illustrates activation thresholds for fiber diameters ranging between 2 and 20 µm. The

simulation is conducted with the MRG model and a single point electrode that is located 10 mm above the middle of a 20 mm long, straight fiber. The resistance of the medium is 35 Ωcm. The stimulation pulse is 1 ms long.

It can be seen that the relationship is not linear and that the activation threshold rapidly increases for small fiber diameters. The relationship can be approximated as the threshold being inverse proportional to the fiber diameter. A linear regression with the activation threshold I_{thr} as the dependent variable and the reciprocal of the fiber diameter $1/d$ as the independent variable results in:

$$I_{thr} = 4.999 - 102.009 \cdot 1/d \tag{3.20}$$

with $R^2 = .988$. Thus $1/d$ can be regarded as proportional to the activation threshold in the range between 2 and 20 µm and can be used to approximate the influence of the change of the activation threshold when the fiber diameter is adjusted in the case of extracellular stimulation.

Intracellular stimulation In intracellular stimulation a reverse relationship to the extracellular case can be observed, small fiber diameters have lower excitation thresholds than larger fibers. For example thresholds for a 2 cm long fiber intracellularly stimulated at the middle node of Ranvier has a threshold of 147, 300 and 599 pA for diameters of 5, 10 and 16 µm, respectively.

Activation threshold and fiber curvature

The curvature of the fiber in the electrical field generated by electrodes has an effect on the activation threshold, since it enhances or reduces the curvature of the extracellular field, evaluated fiber trajectory. And as already discussed (see section 2.3) the activating function, which predicts the excitability of fibers

in an electrical field, is proportional to the second order spatial derivative of the potential field along the fiber. Figure 3.8 illustrates this effect for c values between -1 and 1, c.f. figure 3.2. The electrode to fiber distance is set to 5 mm and the fiber diameter is 16 μm. The threshold was calculated with the electrode being at negative potential.

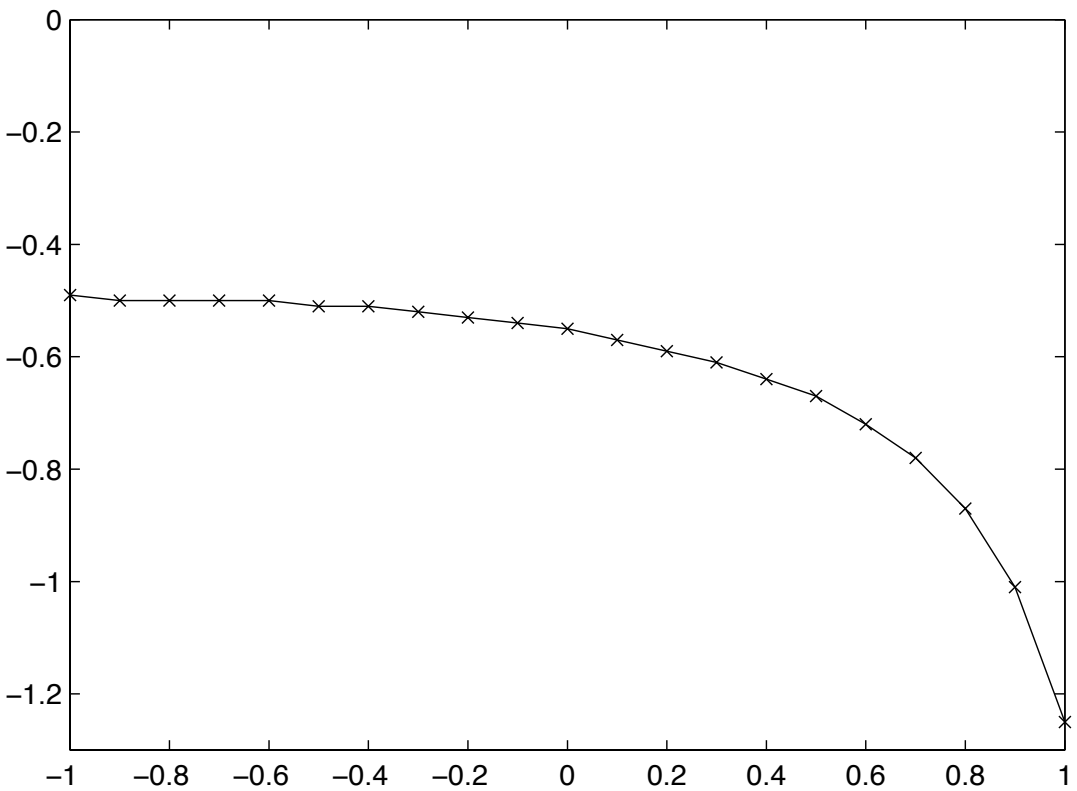

Figure 3.8: Influence of the fiber curvature on the activation threshold. X-axis c value as specified in the *Nerve fiber curvature* field, y-axis activation threshold.

The results show a rather large difference between a straight fiber and a fiber bent (with $c = 1$) towards the electrode, the activation threshold increases to 227.3%. While the decrease of the activation threshold of a fiber bent away from the electrode is only to 89.2%. This can be explained by investigating the electrical field in comparison to the fiber trajectory, for the case of the fiber be-

ing bent towards the electrode with $c = 1$ the electrode position almost matches the center of the circle, the fiber is part of. This results in the isopotential lines of the electrical field, being almost parallel to the fiber geometry and thus there is little change in the potential along the fiber. In order to reduce the threshold further more abrupt changes of the fiber trajectory away from the electrode are needed. Such fiber bendings in combination with transitions of the fiber between two different media are the reason that posterior root fiber can be stimulated transcutaneously Ladenbauer et al. (2010).

Activation threshold and electrode-fiber distance

The distance of the electrode from the fiber strongly influences the activation threshold. This is due to two main properties, first, the electrical field is more focused, when the electrode is near the fiber and thus the activating function reaches pronounced high, second, the absolute values of the potential field decrease the farther away the electrode is from the fiber. Thus, in general, the closer electrode is to a straight fiber the lower the excitation threshold of said fiber. In figure 3.9 the potential distributions and activating functions of two exemplary electrode-fiber distances of 1 and 10 mm are illustrated.

Stimulation functions

Custom stimulation functions can be defined by setting *Stimulation function* to custom and typing a function, depending from `t` into *Custom function.* An example an be seen in figure 3.11.

In figure 3.11 it is noteworthy to point out that the first three action potentials are propagated, although the amplitude of the subsequent action potentials at the node where it is initiated is reduced but the fourth action potential is not being propagated along the the fiber.

Sometimes it is desired to stay current neutral, meaning the sum of the current that is introduced into the medium should be 0. This can be done by using two adjacent pulses, one with negative and one with positive polarity. Especially with implanted electrodes staying current neutral is desired.

To illustrate the effect of the different configurations, the activation thresholds of the a single cathodic pulse (1 ms: -0.548 mA, 0.1 ms: -1.92), a cathodic pulse followed by an anodic pulse (1 ms: 0.554 mA, 0.1 ms: 2.39) and an anodic pulse followed by an cathodic pulse (1 ms: 0.531 mA, 0.1 ms: 2.99) were calculated. All simulations were performed with a straight 16 µm thick fiber and an electrode fiber distance of 5 mm. It can be seen that the threshold is slightly reduced by an anodic pulse followed by a cathodic pulse for the 1 ms pulse duration, while with a pulse duration of 0.1 ms both double-pulse configurations increase the activation threshold significantly.

It is also possible to create custom stimulation functions using m-files. An example is shown in listing 3.4 and illustrated in figure 3.12. The function creates an stimulation function shaped like half of the phase of a sine function with the length as specified by the argument l. The activation threshold of this function is with -0.09 mA only slightly above the activation threshold for the rectangular stimulation pulse, which is -0.07 mA.

Listing 3.4: Custom stimulation function m-file

```
function x = stim( t,length )

    if t < length
        x = sin(t*pi/length);
    else
        x=0;
    end

end
```

Further also custom stimulation functions can make use of the frequency, e.g. when the frequency is set to 1000 Hz, stimulation pulses are directly chained after each other. Also sinusoid high frequency stimulation can be created with custom stimulation functions. An example is shown in figure 3.13 where an 16 µm diameter, straight fiber has been stimulated with 10 kHz stimulation of an extracellular electrode with 0.6 mA peak-to-peak intensity and an electrode-fiber distance of 1 mm. Four action potentials are elicited. Afterwards the the fiber remains 'silent'. No action potentials are elicited, even if the simulation is conducted for a longer time. According to Bhadra, Lahowetz, Foldes, and Kilgore (2007) such high frequency sinusoidal electrical stimulation can create a nerve fiber block. After a setup time all action potentials reaching the stimulated parts will not be able to propagate further.

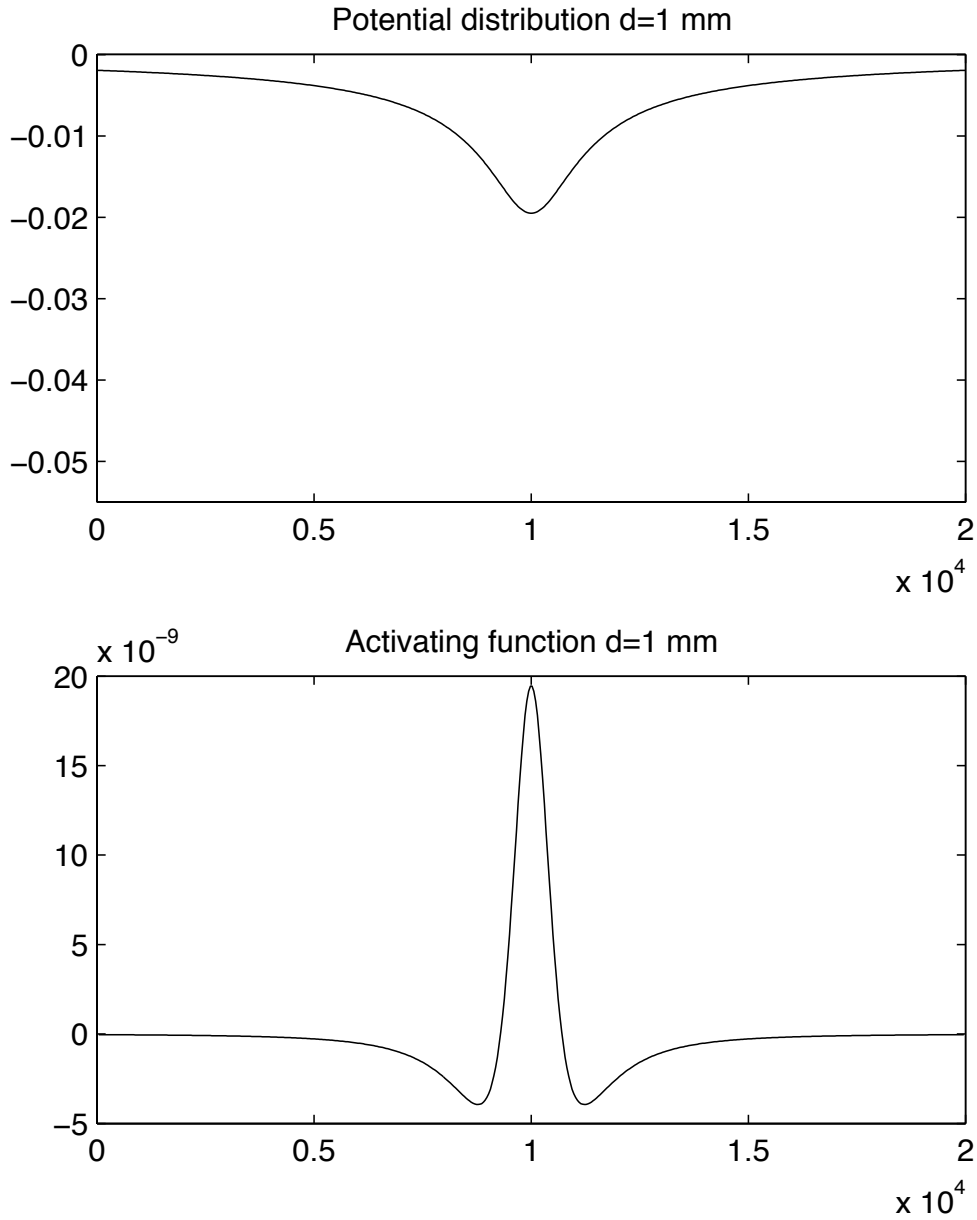

Figure 3.9: Influence of the electrode to fiber distance on the potential distribution and activating function. This figure: 1 mm distance, figure 3.10: 10 mm distance. Electrodes are at the activation thresholds, e.g. -0.07 and -1.95 mA for the 1 and 10 mm fibers, respectively. The focused field with large values of the activating function can be seen on the left, while the absolute potential is higher on the right.

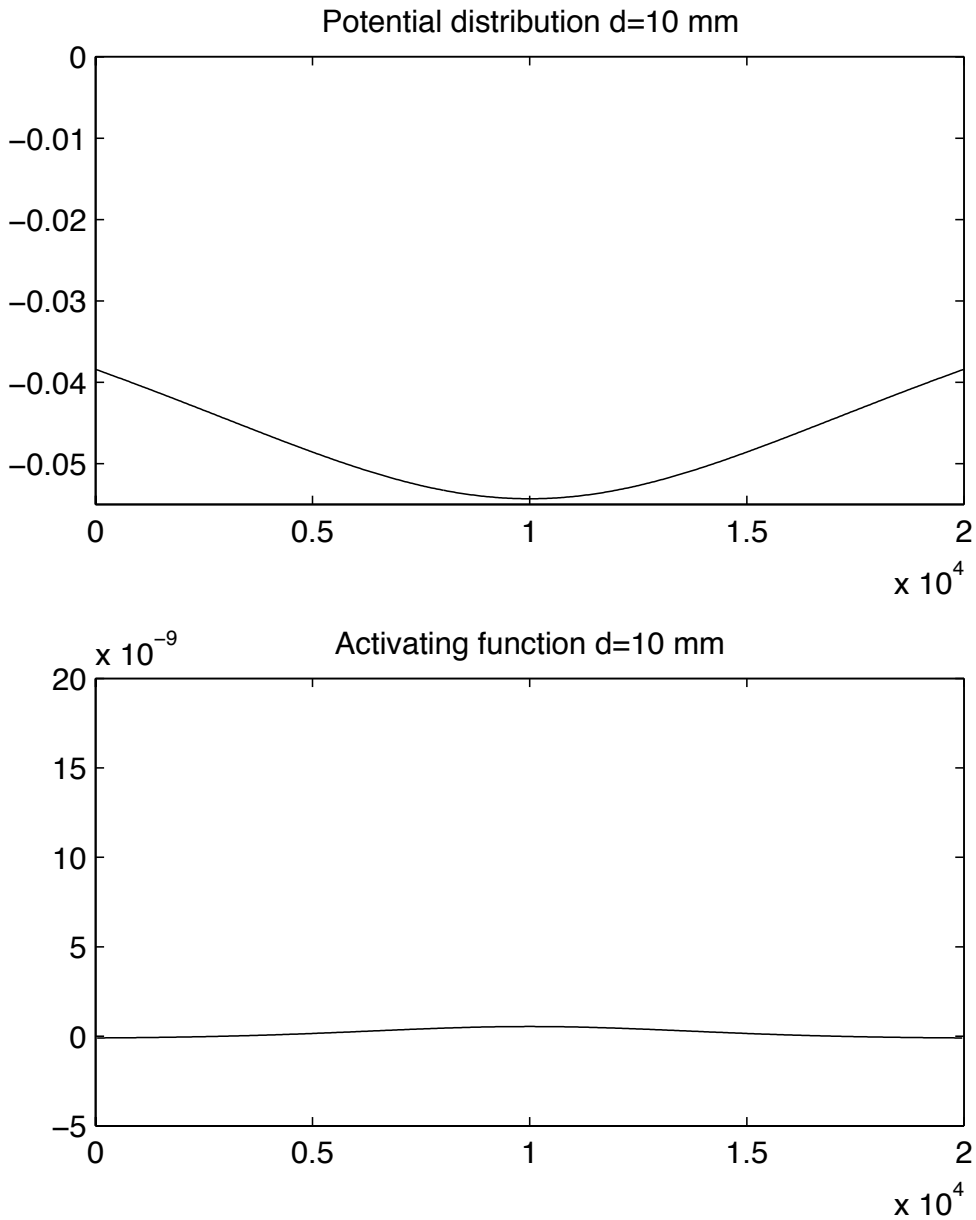

Figure 3.10: See caption figure 3.9.

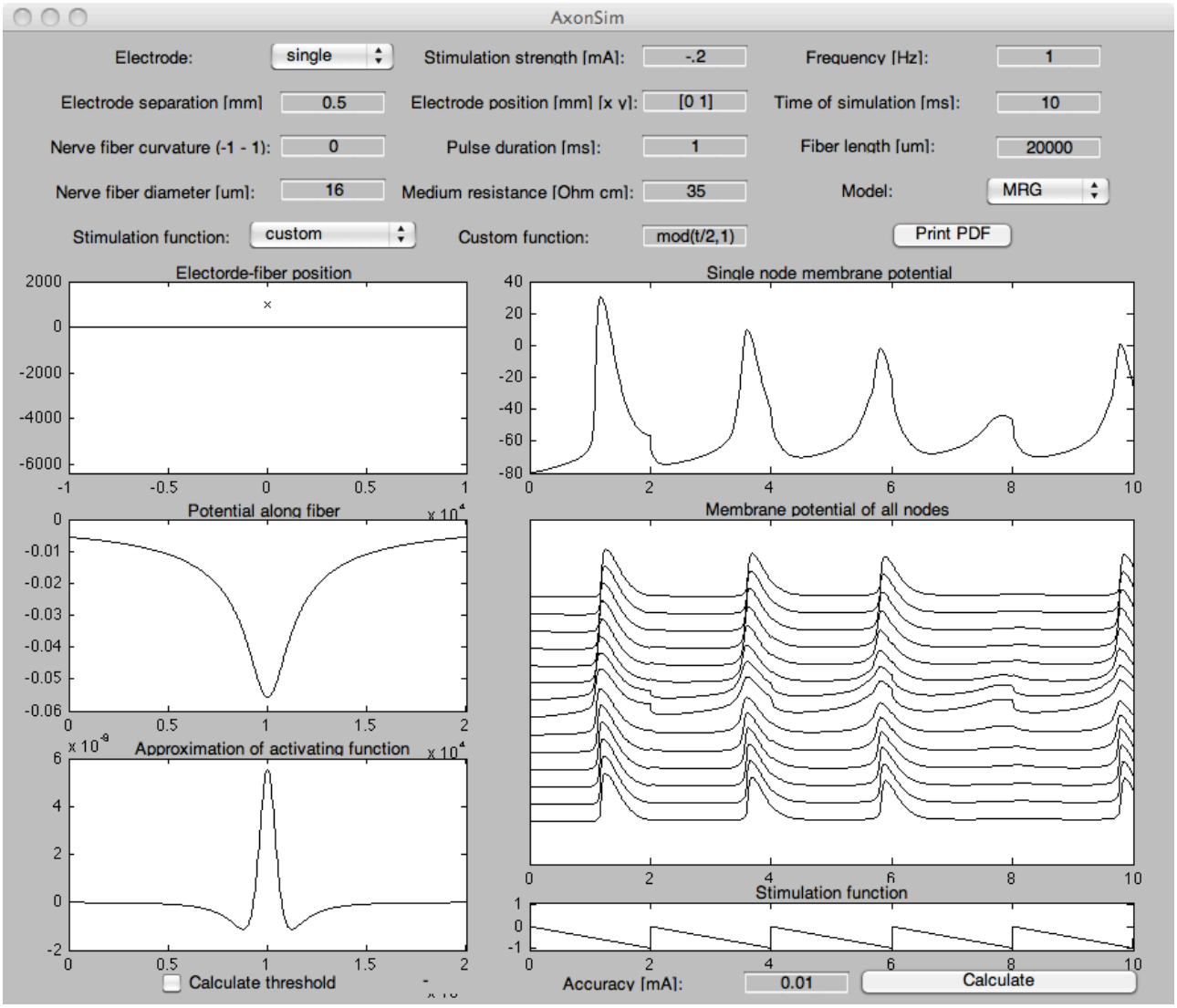

Figure 3.11: Example of a custom stimulation function. The function mod(t/2,1) creates a sawtooth stimulation function with a frequency of 500 Hz.

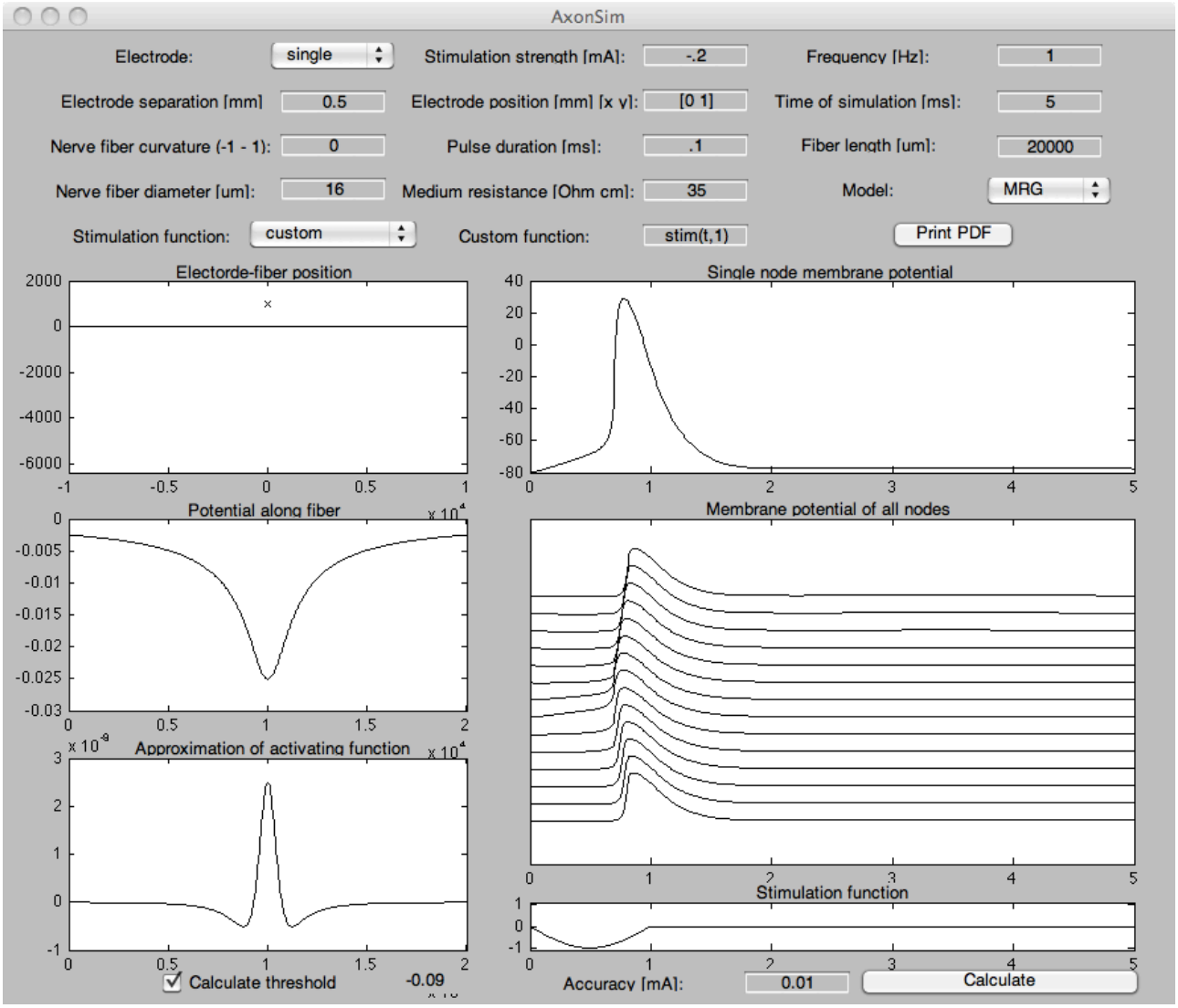

Figure 3.12: Example of a custom stimulation function specified by a function file. The method `stim(t,l)` creates an l ms long stimulation pulse.

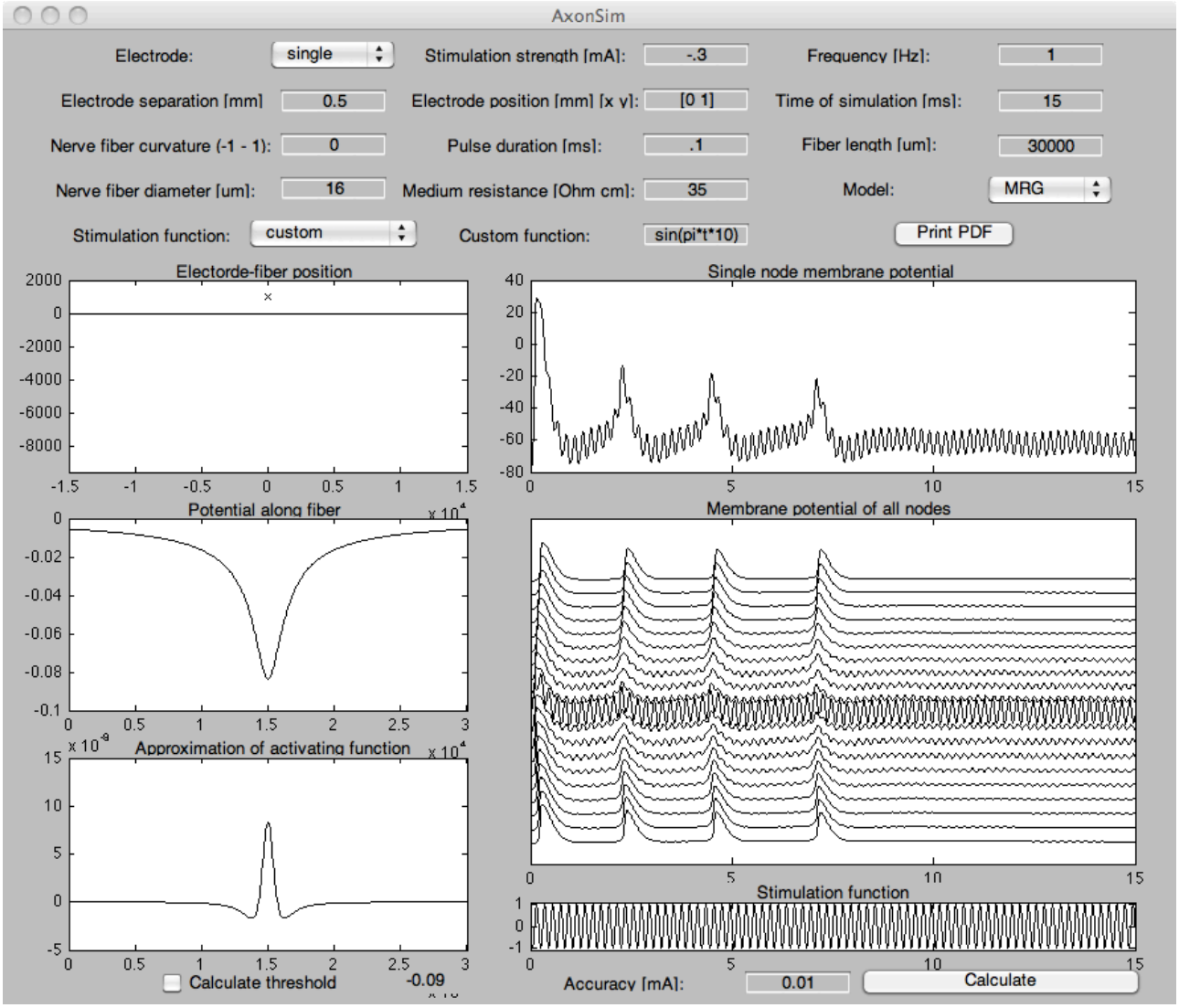

Figure 3.13: Illustration of the effect of 10 kHz stimulation with en extracellular electrode.

Chapter 4

Summary

An application, AxonSim, was presented that can be used to simulate two different nerve fiber models, the McIntyre-Richardson-Grill (MRG) model and the Chiu-Ritchie-Rogart-Stagg-Sweeney (CRRSS) model. Both are commonly used models for the mammalian myelinated axon. The theory behind the nerve fiber models and the electrical stimulation of the nervous system was elaborated. Many features of the electrical stimulation of the nervous system that can be studied with computer models were investigated as examples of use of AxonSim. Further crucial parts of the source code of AxonSim were reviewed and explained.

The presented application, in combination with this text, is well suited to teach the underlying principles of axon models and their behavior under the influence of extra- and intracellular artificial stimulation. Furthermore, the presented application is appropriate to study nerve fiber models without supervision for everyone who wants to get acquainted with the topic, since all kinds of configurations can be simulated and cues are given in the text on how the parameters have an influence on the outcome.

Bibliography

Amassian, V. E. and P. J. Maccabee (2006). Transcranial magnetic stimulation. *Proceedings of the 28th IEEE EMBS Annual International Conference 1*, 1620–1623.

Barrett, E. F. and J. N. Barrett (1982). Intracellular recording from vertebrate myelinated axons: mechanism of the depolarizing afterpotential. *The Journal of Physiology 323*(1), 117–144.

Bear, M. F., B. W. Connors, and M. A. Paradiso (2001). *Neuroscience: Exploring the brain.* Lippincott Williams & Wilkins.

Bhadra, N., E. A. Lahowetz, S. T. Foldes, and K. L. Kilgore (2007). Simulation of high-frequency sinusoidal electrical block of mammalian myelinated axons. *Journal of Computational Neuroscience 22*(3), 313–326.

Calabrese, R. L. and A. A. Prinz (2010). Realistic modeling of small neuronal networks. In E. De Shutter (Ed.), *Computational Modeling Methods for Neuroscientists*, pp. 285–316. MIT Press.

Chiu, S. Y., J. M. Ritchie, R. B. Rogart, and D. Stagg (1979). A quantitative descritpion of membrane currents in rabbit myelinated nerve. *The Journal of Physiology 292*(1), 149–166.

Coburn, B. (1985). A theoretical study of epidural electrical stimulation of the spinal cord - Part II: effects on long fyelinated fibers. *IEEE Transactions on Biomedical Engineering 32*(11), 978–986.

Danner, S. (2010). *Computer simulation of electrically stimulated nerve fibers in the human spinal cord.* Master thesis, Vienna University of Technology.

Danner, S. M. (2011). *An application for learning and teaching extracellular stimulation of axons.* Master thesis, Vienna University of Technology.

Danner, S. M., U. S. Hofstoetter, J. Ladenbauer, F. Rattay, and K. Minassian (2011). Can the human lumbar posterior columns be stimulated by transcutaneous spinal cord stimulation? A modeling study. *Artificial Organs 35*(3), 257–262.

Dayan, P. and L. F. Abbott (2001). *Theoretical neuroscience: Computational and mathematical modeling of neural systems.* MIT Press.

De Shutter, E. (2010). *Computational modeling methods for neuroscientists.* MIT Press.

Dimitrijevic, M. M. and M. R. Dimitrijevic (2002). Clinical elements for the neuromuscular stimulation and functional electrical stimulation protocols in the practice of neurorehabilitation. *Artificial organs 26*(3), 256–9.

Frankenhaeuser, B. and A. F. Huxley (1964). The action potential in the myelinated nerve fibre of Xenopus laevis as computed on the basis of voltage clamp data. *The Journal of Physiology 171*, 302–315.

Grill, W. M. (1999). Modeling the effects of electric fields on nerve fibers: influence of tissue electrical properties. *IEEE Transactions on Biomedical Engineering 46*(8), 918–28.

Halter, J. A. and J. W. Clark (1991). A distributed-parameter model of the myelinated nerve fiber. *Journal of Theoretical Biology 148*(3), 345–82.

Hindmarsh, A. C., P. N. Brown, K. E. Grant, S. L. Lee, R. Serban, D. E. Shumaker, and C. S. Woodward (2005). SUNDIALS: Suite of nonlinear and differential/algebraic equation solvers. *ACM Transactions on Mathematical Software (TOMS) 31*(3), 363–396.

Hodgkin, A. L. and A. F. Huxley (1952). A quantitaive description of membrane current and its application to conduction and excitation in nerve. *The Journal of Physiology 117*(4), 500–544.

Iles, J. F. (2005). Simple models of stimulation of neurones in the brain by electric fields. *Progress in Biophysics and Molecular Biology 87*, 17–31.

Izhikevich, E. M. (2003). Simple model of spiking neurons. *IEEE Transactions on Neural Networks 14*, 1569–1572.

Izhikevich, E. M. (2006). Polychronization: Computation with spikes. *Neural Computation 18*, 245–282.

Izhikevich, E. M. (2007). *Dynamical systems in neuroscience: The geometry of excitability and bursting.* MIT Press.

Kandel, E. R., J. H. Schwartz, and T. M. Jessell (2000). *Principles of neural science.* McGraw-Hill.

Kuhn, A. (2008). *Modeling transcutaneous electrical stimulation.* Ph. D. thesis, ETH Zürich.

Kuhn, A., T. Keller, M. Lawrence, and M. Morari (2009). A model for transcutaneous current stimulation: simulations and experiments. *Medical & Biological Engineering & Computing 47*(3), 279–89.

Ladenbauer, J. (2008). *Simulation of the excitation of human lower spinal cord structures with surface electrodes : 3D finite element analysis and nerve fiber modeling.* Master thesis, Vienna University of Technology.

Ladenbauer, J., K. Minassian, U. Hofstoetter, M. Dimitrijevic, and F. Rattay (2010). Stimulation of the human lumbar spinal cord with implanted and surface electrodes: a computer simulation study. *IEEE Transactions on Neural Systems and Rehabilitation Engineering 18*(6), 637–645.

Lapicque, L. (1907). Recherches quantitatives sur l'excitation électrique des nerfs traitée comme une polarization. *Journal de physiologie et de pathologie générale 9*, 620–635.

Liberson, W. T., H. J. Holmquest, D. Scot, and M. Dow (1961). Functional electrotherapy: stimulation of the peroneal nerve synchronized with the swing phase of the gait of hemiplegic patients. *Archives of Physical Medicine and Rehabilitation 42*, 101–5.

Maass, W. and C. M. Bishop (2001). *Pulsed neural networks.* MIT Press.

Maccabee, P. J., V. E. Amassain, L. P. Eberle, and R. Q. Cracco (1993). Magnetic coil stimulation of straight and bent amphibian and mammalian peripheral nerve in bitro: locus of excitation. *Journal of Physiology 460*, 201–219.

McIntyre, C. C., W. M. Grill, D. L. Sherman, and N. V. Thakor (2004). Cellular effects of deep brain stimulation: model-based analysis of activation and inhibition. *Journal of Neurophysiology 91*(4), 1457–69.

McIntyre, C. C., A. G. Richardson, and W. M. Grill (2002). Modeling the excitability of mammalian nerve fibers: influence of afterpotentials on the recovery cycle. *Journal of Neurophysiology 87*(2), 995–1006.

McNeal, D. R. (1976). Analysis of a model for excitation of myelinated nerve. *IEEE Transactions on Biomedical Engineering 23*(4), 329–37.

Minassian, K., I. Persy, F. Rattay, M. R. Dimitrijevic, C. Hofer, and H. Kern (2007). Posterior root-muscle reflexes elicited by transcutaneous stimulation of the human lumbosacral cord. *Muscle & Nerve 35*(3), 327–36.

Niebur, E. (2008). Neuronal cable theory. *Scholarpedia 3*, 2674.

Nowak, L. G. and J. Bullier (1998). Axons, but not cell bodies, are activated by electrical stimulation in cortical gray matter. II. Evidence from selective inactivation of cell bodies and axon initial segments. *Experimental brain research. 118*(4), 489–500.

Pfützner, H. (2003). *Angewandte Biophysik.* Wien-New York: Springer.

Porter, R. (1963). Focal stimulation of hypoglossal neurones in the cat. *The Journal of Physiology 169*(3), 630.

Ranck, J. B. J. (1975). Which elements are excited in electrical stimulation of mammalian central nervous system: A review. *Brain Research 98*, 417–440.

Rattay, F. (1986). Analysis of models for external stimulation of axons. *IEEE Transactions on Biomedical Engineering 33*(10), 974–977.

Rattay, F. (1987). Ways to approximate current-distance relations for electrically stimulated fibers. *Journal of Theoretical Biology 125*(3), 339–49.

Rattay, F. (1988). Modeling the excitation of fibers under surface electrodes. *IEEE Transactions on Biomedical Engineering 35*(3), 199–202.

Rattay, F. (1989). Analysis of models for extracellular fiber stimulation. *IEEE Transactions on Biomedical Engineering 36*(7), 676–82.

Rattay, F. (1990). *Electrical nerve stimulation.* Wien-New York: Springer Verlag.

Rattay, F. (1998). Analysis of the electrical excitation of CNS neurons. *IEEE Transactions on Biomedical Engineering 45*(6), 766–72.

Rattay, F. (1999). The basic mechanism for the electrical stimulation of the nervous system. *Neuroscience 89*(2), 335–346.

Rattay, F. and M. Aberham (1993). Modeling axon membranes for functional electrical stimulation. *IEEE Transactions on Biomedical Engineering 40*(12), 1201–1209.

Rattay, F., R. J. Greenberg, and S. Resatz (2003). Neuron modeling. In W. E. Finn and P. G. LoPresti (Eds.), *Handbook of Neuroprosthetic Methods*, pp. 39–71.

Rattay, F., K. Minassian, and M. R. Dimitrijevic (2000). Epidural electrical stimulation of posterior structures of the human lumbosacral cord: 2. quantitative analysis by computer modeling. *Spinal Cord 38*(8), 473–89.

Rattay, F. and C. Wenger (2010). Which elements of the mammalian central nervous system are excited by low current stimulation with microelectrodes? *Neuroscience 170*(2), 399–407.

Richardson, A. G., C. C. McIntyre, and W. M. Grill (2000). Modelling the effects of electric fields on nerve fibres: influence of the myelin sheath. *Medical & Biological Engineering & Computing 38*(4), 438–46.

Roth, B. J. (1994). Mechanisms for electrical stimulation of excitable tissue. *Critical Reviews in Biomedical Engineering 22*(3-4), 253–305.

Struijk, J. J., J. Holsheimer, and H. B. K. Boom (1993). Excitation of dorsal root fibers in spinal cord stimulation: A theoretical study. *IEEE Transactions on Biomedical Engineering 40*(7), 632–639.

Sweeney, J. D., J. T. Mortimer, and D. Durand (1987). Modeling of mammalian myelinated nerve for functional neuromuscular electrostimulation. *Proceedings of the 97h Annual Conference IEEE EMBS*, 1577–1578.

Száva, Z., S. M. Danner, and K. Minassian (2011). *Transcutaneous electrical spinal cord stimulation: Biophysics of a new rehabilitation method after spinal cord injury.* Saarbrücken: VDM Verlag Dr. Müller.

Veltink, P. H., J. A. van Alsté, and H. B. Boom (1988). Simulation of intrafascicular and extraneural nerve stimulation. *IEEE Transactions on Biomedical Engineering 35*(1), 69–75.

Warman, E. N., W. M. Grill, and D. Durand (1992). Modeling the effects of electric fields on nerve fibers: determination of excitation thresholds. *IEEE Transactions on Biomedical Engineering 39*(12), 1244–54.

Wenger, C., L. Paredes, and F. Rattay (2011). Current-distance relations for microelectrode stimulation of pyramidal cells. *Artificial Organs 35*(3), 263–266.

Wesselink, W. A., J. Holsheimer, and H. B. Boom (1999). A model of the electrical behaviour of myelinated sensory nerve fibres based on human data. *Medical & Biological Engineering & Computing 37*(2), 228–235.

Wongsarnpigoon, M. and W. M. Grill (2008). Computational modeling of epidural cortical stimulation. *Journal of Neural Engineering 5*, 443–454.